STATISTICAL ESTIMATION OF CASCADING BLACKOUT SIZE AND PROPAGATION WITH BRANCHING PROCESSES

by

Kevin R. Wierzbicki

A thesis submitted in partial fulfillment of
the requirements for the degree of

Master of Science

(Electrical and Computer Engineering)

at the

UNIVERSITY OF WISCONSIN–MADISON

2006

ACKNOWLEDGMENTS

I would like to thank Professor Ian Dobson for his guidance, insight, and most importantly for the opportunity to participate in this research. I also gratefully acknowledge support in part from NSF grant ECS-0214369 and the Power Systems Engineering Research Center (PSERC).

DISCARD THIS PAGE

TABLE OF CONTENTS

Page

DISCARD THIS PAGE

LIST OF TABLES

DISCARD THIS PAGE

LIST OF FIGURES

Appendix
Figure Page

ABSTRACT

Cascading blackouts on a bulk power transmission system are potentially catastrophic events with a large impact on society characterized by a sequence of line trips and load shed. One spectacular example of a cascading blackout is the August 2003 blackout in North America that affected 50 million people. We propose using branching processes to model the line tripping and load shed behavior of cascading blackouts. We use an estimator of the offspring mean, λ, to fit simulated blackout data to the branching process model. The parameter λ is a measure of cascade propagation, and helps us to estimate how likely large blackouts are. We compute distributions of blackout size and total number of line failures from the model and match them against simulated data. The match with simulated data suggests that the branching process model captures important aspects of the cascade phenomenon. The line failures and load shed in cascades are seen to have similar λ, meaning they propagate at the same rate. The branching process model is an efficient way to estimate line failure and load shed probability distributions.

Chapter 1

Introduction

A cascading blackout is one in which a contingency or set of contingencies cause a cascading series of further failures to propagate across a power grid. The "domino effect" is a useful heuristic for this phenonemon. For an example of how devastating a cascading blackout can be, look no further than the August 2003 blackout that affected Eastern Canada and the Northeastern United States. This event resulted in about 50 million people without electricity and over $6 billion in financial losses [39, 19].

We focus on using a simple statistical mathematical model of a cascade to predict how likely a cascading blackout is for a given system. By performing statistical analysis on previous blackout data, we can fit the prior data to a model and generate a probability density function (pdf) of blackout sizes. Then it will be known how likely a cascading blackout of a certain size will be in the future, if one would happen to start. Also, the model gives important information about how "close" a power system is to a cascading regime even if large cascades have not happened recently.

It has been shown that a simple model of cascading failure can be approximated well by a particular mathematical model called a branching process [15]. This has motivated using branching processes to model various aspects of a cascading blackout. Branching processes have been used to describe various "cascading" type events such as epidemics [2], and earthquakes [35], as well as more abstract cases such as perseverance of family names [26]. Their mathematical properties have been widely studied, with the best sources being [26, 1, 28]. Branching processes of some form can potentially be applied to any type of cascading phenomenon, so it is natural to extend them to blackouts.

For our purposes, we use branching processes to model both line outages and load shed produced by a cascading blackout. Discrete state branching processes are used for line failures, with the mathematics presented in Section 2.1. Continuous state branching processes are used for load shed, with the mathematics presented in Section 2.2. The model specifies a sequence of failures at discrete stages n, with failures at stage n causing further failures at stage $n+1$. The most interesting aspect of the modeling is the propagation factor λ which captures the potential of the cascade to either die out or grow, and thus governs the likely size of the cascade. When $\lambda < 1$, the cascade is likely to die out, while when $\lambda > 1$ it is likely to become large. λ is also the mean of the offspring distribution, which is the distribution of failures at stage $n+1$ caused by a single failure, or unit of failure, at stage n. Once the offspring distribution is specified, the distribution of the total amount, or number of failures is produced. In the case of line failures, this is total number of lines tripped (taken out of service) during the cascade. In the case of load shed, this is the total amount of system load demand that is removed as a result of the cascade.

To fit the model to a particular power system simulation, all parameters needed by the branching process model including λ must be estimated from previous blackout data. A history of blackout sizes and line failures must be available for previous blackouts. Moreover, they must be available in sequential, time-ordered form. Section 3 shows the methods used to fit both line failure and load shed data.

Constructing blackout and failure distributions by way of a branching process model is much more efficient than simply constructing empirical distributions from historical data. λ can be accurately estimated using a relatively small amount of data.

We test our methods on the OPA power system model [6], using the IEEE 118 bus test system. The OPA model uses DC load flow and LP dispatch. Cascades are initiated by overloading the system so that lines are tripped. This initiating event may cause further line failures, and load shed as the system redispatches. The simulation is run multiple times for various loading levels simulating a history of cascades. The procedures of Section 3 are used to gain estimates of λ and other relevant parameters. The distributions are then plotted and compared to the

empirical data to test the accuracy of the model. A description of OPA, as well as results for line failures and load shed, are presented in Section 4.

1.1 Literature Review

This section is divided up into two parts. The first briefly describes the literature directly related to this thesis. The second describes literature not directly related to this project but related to cascading blackouts.

1.1.1 Branching Processes with Power Systems

Using branching processes to model cascading failures in power systems was first proposed by Dobson et al in [15]. That work was an extension of the CASCADE model shown in [18, 13]. CASCADE is a simple, abstracted model of cascading failures. It is shown in [15] that under certain limiting conditions, CASCADE can be approximated by a branching process. Applying branching processes to OPA power system simulation data was then done in [17] and [47] as a part of this project.

1.1.2 Additional Cascading Blackout Research

Work on cascading blackouts can be divided into three categories: modeling, mitigation, and miscellaneous. "Modeling" refers to any simple or complex abstraction of cascading failure to gain understanding of the phenomenon. This model can be used to predict behavior of real power systems in cascading regimes. This project falls into this category. In [8], Q. Chen and McCalley use a cluster model to construct probability distributions of line failures. Their use of a parameter α to represent the tendency of failures to "cluster" is similar to our use of λ to describe the tendency of failures to propagate. Carreras et al show in [7] show that power-law tails are present in blackout data. They conjecture that the power-laws are due to Self-Organized Criticality of the power system and explore this possibility through the OPA power system model in [6]. The OPA model simulates the long-term dynamics of a power system as generation and transmission lines are upgraded in response to cascading blackouts and

growing demand. In [9], J. Chen et al use a hidden failure model to estimate cascade blackout sizes. The hidden failures refer to incorrect relay tripping which has been observed in real systems. Roy et al develop generic network models in [34] that represent large, interconnected complex systems capable of cascading failure. They simulate random network growth, noting the distribution of connections, and employ a Markov model of network failure.

"Mitigation" refers to techniques that can be used by power system operators to stop cascades from spreading. In [43], Venkatasubramanian and Quintero suggest using Static-Var-Compensator (SVC) control techniques to dampen growing oscillations in a power system. Through central control, the SVCs would be able to quickly react to stop oscillations and restore the system to normal operation before cascading failures cripple the system. In [44] Vittal and Wang use a forced islanding scheme to separate parts of a power system before a cascading failure can grow. These mitigation methods have the property of being "on-line," that is they are used when a cascading failure is thought to be occurring.

"Miscellaneous" can be any cascading failure research that does not fit into the above two categories. For example, in [25], Hardiman et al describe their TRELSS simulation, used to simulate power system response to a variety of contingencies. They also give a brief overview of some recent cascading blackouts. Kirschen et al use variance reduction Monte Carlo techniques in [29] to estimate stress on a power system.

Chapter 2

Branching Processes

2.1 Discrete State Branching Process

This section explains discrete state branching processes to the detail necessary for this project. See [26, 1] for more information.

In the discrete state branching process, a cascade starts with an initial number of failures X_0 and proceeds to produce a sequence of failures $X_1, X_2, \ldots$, at discrete stages $n = 0, 1, 2, \ldots$. The failures at each stage are nonnegative integers so $X_n \in Z^{\geq 0}$ and X_n can be seen as the number of lines failed at stage n in a cascade. The offspring distribution $P[X = x]$ is defined to be the distribution function of failures at stage $n + 1$ resulting from one failure at stage n, as well as the distribution of a random variable X with mean λ and probability generating function

$$f(s) = \mathrm{E}[s^X] = \sum_{i=0}^{\infty} P[X = i]s^i,$$

and where $P[X = 0] > 0$. Combining these definitions gives

$$P[X_{n+1} = x \,|\, X_n = 1] = P[X = x].$$

When the initial number of failures X_0 is given by a constant then the number of failures X_1 at stage 1 is distributed as a sum of X_0 independent copies of X:

$$X_1 \stackrel{d}{=} \sum_{i=1}^{X_0} X.$$

In general, X_{n+1} is distributed as a sum of X_n independent copies of X:

$$X_{n+1} \stackrel{d}{=} \sum_{i=1}^{X_n} X.$$

In terms of generating functions, this becomes

$$f_{n+1}(s) = \mathrm{E}[s^{X_{n+1}}] = \mathrm{E}[\mathrm{E}[s^{X_{n+1}}|X_n]] = \mathrm{E}[f(s)^{X_n}] = f_n(f(s)), \tag{2.1}$$

where f_{n+1} is the generating function of X_{n+1}.

When the number of initial failures X_0 is a constant, then

$$f_0(s) = \mathrm{E}[s^{X_0}] = s^{X_0}. \tag{2.2}$$

(2.1) and (2.2) imply

$$f_n(s) = \left(f^n(s)\right)^{X_0}, \tag{2.3}$$

where f^n is the n-fold functional composition of f.

As the cascade proceeds, the failures accumulate and the running total of the failures at stage n is given by

$$Y_n = X_0 + X_1 + \ldots + X_n.$$

The average number of failures at each stage is

$$\mathrm{E}X_n = X_0\lambda^n, \tag{2.4}$$

while the average running number of failures is

$$\mathrm{E}Y_n = X_0 \sum_{i=1}^{n} \lambda^n. \tag{2.5}$$

If $\lambda < 1$, the cascade shrinks on average and eventually dies out with probability 1, and Y_n converges to the total

$$Y = \lim_{n\to\infty} Y_n.$$

Assuming the subcritical case $\lambda < 1$, the distribution of Y can be computed from the offspring distribution. Let $F(s)$ stand for the generating function of Y when $X_0 = 1$. In this case,

$$\begin{aligned} F(s) &= \mathrm{E}[s^Y] \\ &= \mathrm{E}[s^{1+X_1+X_2+\cdots}] \\ &= \mathrm{E}[s\mathrm{E}[s^{X_1+X_2+\cdots}|X_1]] \\ &= \mathrm{E}[sF(s)^{X_1}] \\ &= sf(F(s)). \end{aligned} \tag{2.6}$$

Equation (2.6) is then solved implicitly for $F(s)$ using a Lagrange inversion method:

$$F(s) = \sum_{a=1}^{\infty} P[Y = a]s^a = \sum_{a=1}^{\infty} \left(\frac{1}{a!} \frac{d^{a-1}}{dz^{a-1}} \left(f(z)\right)^a \Big|_{z=0} \right) s^a. \tag{2.7}$$

See Section 7.1 for details of the Lagrange inversion method.

If the initial number failures X_0 is randomly chosen according to some distribution $P[X_0 = x]$ with generating function $m(s)$, and mean θ, then (2.2) becomes

$$f_0(s) = m(s)$$

and (2.3) becomes

$$\begin{aligned} f_n(s) &= \mathrm{E}[s^{X_n}] \\ &= \mathrm{E}[\mathrm{E}[s^{X_n}|X_0]] \\ &= \mathrm{E}[(f^n(s))^{X_0}] \\ &= m\left(f^n(s)\right). \end{aligned}$$

Similarly, the generating function of Y becomes $\mathcal{F}(s)$ where

$$\mathcal{F}(s) = m\left(F(s)\right). \tag{2.8}$$

Finally, (2.4) becomes

$$\mathrm{E}X_n = \theta\lambda^n.$$

2.2 Continuous State Branching Processes

This section explains the mathematics of continuous state branching processes that are used in this project. See [28, 36] for more information.

As in the discrete case, continuous state branching process starts with an initial number of failures X_0 and proceeds to produce a sequence of failures $X_1, X_2, \ldots,$ at discrete stages $n = 0, 1, 2, \ldots$. The failures at each stage are, this time, nonnegative real numbers so that $X_n \in \mathcal{R}^{\geq 0}$ and X_n can be seen as the amount of load shed at stage n in a cascade. The offspring

distribution $H(x)$ is defined to be the distribution function of failures at stage $n+1$ resulting from one failure at stage n. $H(x)$ is the probability density function of a nonnegative, infinitely divisible continuous random variable X with mean λ, and cumulant generating function

$$h(s) = -\ln \mathrm{E}[e^{-sX}] = -\ln \int_0^\infty e^{-sx} H(x) dx.$$

When the initial number of failures X_0 is given by a constant then the number of failures X_1 at stage 1 is distributed as a sum of X_0 independent copies of X:

$$X_1 \stackrel{d}{=} \sum_{i=1}^{X_0} X. \tag{2.9}$$

In general, X_{n+1} is distributed as a sum of X_n independent copies of X:

$$X_{n+1} \stackrel{d}{=} \sum_{i=1}^{X_n} X. \tag{2.10}$$

In terms of generating functions, this becomes

$$\begin{aligned} h_{n+1}(s) &= -\ln \mathrm{E}[e^{-sX_{n+1}}] \\ &= -\ln \mathrm{E}[\mathrm{E}[e^{-sX_{n+1}}|X_n]] \\ &= -\ln \mathrm{E}\left[\left(\mathrm{E}[e^{-sX}]\right)^{X_n}\right] \\ &= -\ln \mathrm{E}\left[e^{-\left(-\ln \mathrm{E}e^{-sX}\right)X_n}\right] \\ &= h_n(h(s)), \end{aligned}$$

where h_{n+1} is the generating function of X_{n+1}, hence

$$h_n(s) = h_0(h^{(n)}(s)),$$

where $h^{(n)}$ is the n-fold functional composition of h.

When the initial failures X_0 is a constant, then

$$h_0(s) = X_0 s$$

and

$$h_n(s) = X_0 \left(h^{(n)}(s)\right). \tag{2.11}$$

In the continuous case, (2.9) and (2.10) usually describe nonintegral sums of random variables. The way around this conceptual (and mathematical) difficulty is to require the offspring distribution $H(x)$ to be infinitely divisible so that, by definition:

$$X \stackrel{d}{=} \sum_{i=1}^{k} T_k^{(i)}$$

for some i.i.d. random variables $T_k^{(i)}$ and arbitrary integer k.(note: this is definition of infinite divisibility ([22])) Then, (2.9) can be rewritten

$$\begin{aligned} X_1 &\stackrel{d}{=} \sum_{i=1}^{X_0} X^{(i)} \\ &\stackrel{d}{=} \lim_{k\to\infty} \sum_{i=1}^{\lfloor kX_0 \rfloor} T_k^{(i)}. \end{aligned}$$

For example, in the case $X_0 = 2.5$, X_1 becomes

$$\begin{aligned} X_1 &\stackrel{d}{=} \sum_{i=1}^{2.5} X^{(i)} \\ &\stackrel{d}{=} \sum_{i=1}^{25} T_{10}^{(i)} \end{aligned}$$

The running total of load shed at stage n is again given by

$$Y_n = X_0 + X_1 + \ldots + X_n.$$

The average number of failures at each stage is again (2.4) while the average running number of failures is (2.5). If $\lambda < 1$, the cascade shrinks on average and eventually dies out with probability 1, and Y_n converges to the total

$$Y = \lim_{n\to\infty} Y_n.$$

Assuming the subcritical case $\lambda < 1$, the distribution of Y can be computed from the offspring distribution. Let $k(s)$ stand for the cumulant generating function of Y when $X_0 = 1$. In this

case,

$$\begin{aligned} k(s) &= -\ln \mathrm{E}[e^{-sY}] \\ &= -\ln \mathrm{E}[e^{-s(1+X_1+X_2+\ldots)}] \\ &= -\ln \mathrm{E}[e^{-s}\mathrm{E}[e^{-s(X_1+X_2+\ldots)}|X_1]] \\ &= -\ln \mathrm{E}[e^{-s}e^{-k(s)X_1}] \\ &= s + h(k(s)). \end{aligned} \tag{2.12}$$

Equation (2.12) is then solved implicitly for $k(s)$ using the Lagrange expansion (see Section 7.1)

$$k(s) = s + \sum_{a=1}^{\infty} \frac{1}{a!} \frac{d^{a-1}}{ds^{a-1}} (h(s))^a. \tag{2.13}$$

If the initial number failures X_0 is randomly chosen according to some distribution $M(x)$ with cumulant generating function $m(s)$, and mean θ, then (2.11) becomes

$$h_n(s) = m\left(h^n(s)\right).$$

Similarly, the generating function of Y becomes $\mathcal{K}(s)$ where

$$\mathcal{K}(s) = m\left(k(s)\right). \tag{2.14}$$

Finally, equation (2.4) becomes

$$\mathrm{E}X_n = \theta\lambda^n.$$

Once $\mathcal{K}(s)$ has been obtained, the pdf $K(s)$ of the total load shed Y is obtained as the inverse Laplace transform of $e^{-\mathcal{K}(s)}$ using the Post-Widder method:

$$K(x) = \lim_{a\to\infty} \frac{(-1)^a}{a!} \left(\frac{a}{x}\right)^{a+1} \left(\frac{d^a}{ds^a} e^{-\mathcal{K}(s)} \Big|_{s=a/x} \right). \tag{2.15}$$

The cumulative distribution function is similarly obtained as the inverse Laplace transform of $e^{-\mathcal{K}(s)}/s$. See Section 7.2 for details of the Post-Widder method.

2.2.1 Saturation

In real power systems, the cascade size is limited by the total number of lines in the system. There may also be effects present that tend to inhibit the size of the cascade. We refer to both of these limitations as "saturation," and are included when applying a discrete state branching process to line outages. The simplest way to accomplish this is to assume saturation can be modeled by a single parameter S. Then the total number of line failures must not progress beyond this number, or in other words, $Y \leq S$. The distribution (2.8) must then have all probability mass greater than S transferred to $Y = S$. We have not yet considered how to model saturation effects for load shed.

In the case that $\lambda > 1$, the cascade grows on average and there is a nonzero probability that the cascade grows to $Y = \infty$. In this case, a pdf cannot be defined for Y unless the cascade is forced to stop somewhere. Including saturation solves this problem. It is possible when $\lambda < 1$ for a cascade to reach S as well, although if S is sufficiently large, this happens with low probability.

If the initial line failures θ is large enough, it may be the case that cascades saturate at the initial stage. If this is the case, the line failures initial distribution $P[X_0 = x]$ would have to be modified to include saturation.

Chapter 3

Estimation of Branching Process Parameters

This section details how both blackout and line failure data can be fit to branching processes. Line failure data is fit to a discrete state branching process, while load shed data is fit to a continuous state branching process. The propagation parameter λ and the distribution of the total cascade size Y are estimated in each case.

3.1 Line Failures

A cascading failure simulation is assumed to produce a list of cascading blackouts and for each blackout the number of line failures as well as the failures at each intermediate stage of the blackout is recorded. Specifically there are J separate cascades, and X_n^i denotes the line failures at stage n of cascade i. The accumulated data then looks like this:

$$\begin{array}{lccccc} & \text{stage } 0 & \text{stage } 1 & \text{stage } 2 & \cdots \\ \text{cascade } 1 & X_0^{(1)} & X_1^{(1)} & X_2^{(1)} & \cdots \\ \text{cascade } 2 & X_0^{(2)} & X_1^{(2)} & X_2^{(2)} & \cdots \\ \vdots & \vdots & \vdots & \vdots & \vdots \\ \text{cascade } J & X_0^{(J)} & X_1^{(J)} & X_2^{(J)} & \cdots \end{array} . \tag{3.1}$$

Likewise, $Y_n^{(i)}$ refers to the cumulative failures

$$Y_n^{(i)} = X_0^{(i)} + X_1^{(i)} + \ldots + X_n^{(i)}$$

at stage n of cascade i.

The data must be handled in such a way that each cascade starts with a nonzero number of failures. For example, cascades with no failures are discarded. One effect of this is that the

computed distribution of failures is conditioned on the cascade starting. Each cascade will not necessarily have the same number of stages. $N(i)$ refers to the number of stages of cascade i, with $N(i)$ being determined either by the maximum number of simulated stages being reached, or the cascade hitting the saturation size S. $N(i)$ is thus given by

$$N(i) = \max\left\{ n \;\middle|\; Y_n^{(i)} < S \text{ and } X_{n-1}^{(i)} > 0 \text{ and } n \leq N_{\max} \right\}. \tag{3.2}$$

$N_{\max}$ is the maximum number of stages produced by the simulation.

3.1.1 Estimating λ

The estimator for the propagation λ is

$$\begin{aligned} \hat{\lambda} &= \frac{\sum_{i=1}^{J} \left(X_1^{(i)} + X_2^{(i)} + \ldots + X_{N(i)}^{(i)} \right)}{\sum_{i=1}^{J} \left(X_0^{(i)} + X_1^{(i)} + \ldots + X_{N(i)-1}^{(i)} \right)} \\ &= \frac{\sum_{i=1}^{J} Y_{N(i)}^{i} - X_0^{(i)}}{\sum_{i=1}^{J} Y_{N(i)-1}^{(i)}}. \end{aligned} \tag{3.3}$$

The estimator (3.4) is a variant of the maximum likelihood estimator

$$\frac{\sum_{i=1}^{J} Y_N^i - X_0^{(i)}}{\sum_{i=1}^{J} Y_{N-1}^{(i)}} \tag{3.4}$$

when each cascade has the same number of stages N. (3.4) is consistent and asymptotically unbiased as $J \to \infty$ [11, 24].

The mean of $\hat{\lambda}$ is given by

$$\begin{aligned}
\mathrm{E}\,\hat{\lambda} &= \mathrm{E}\left[\frac{\sum_{i=1}^{J}\left(Y_{N(i)}^{(i)} - X_0^{(i)}\right)}{\sum_{i=1}^{J} Y_{N(i)-1}^{(i)}}\right] \\
&= \sum_{N_i,y_i,x_i} \mathrm{E}\left[\frac{\sum_{i=1}^{J}\left(Y_{N(i)}^{(i)} - X_0^{(i)}\right)}{\sum_{i=1}^{i} Y_{N(i)-1}^{(i)}}\,\middle|\, A\right] P\left(A\right) \\
&= \sum_{N_i,y_i,x_i} \mathrm{E}\left[\frac{\sum_{i=1}^{J}\left(y_i + x_i + X_{N_i}^{(i)} - X_0^{(i)}\right)}{\sum_{i=1}^{J}\left(y_i + x_i\right)}\,\middle|\, A\right] P\left(A\right) \\
&= \sum_{N_i,y_i,x_i} \left(1 + \frac{\sum_{i=1}^{J}(\lambda x_i - X_0^{(i)})}{\sum_{i=1}^{J}(y_i + x_i)}\right) P\left(A\right) \\
&= 1 + \lambda \mathrm{E}\left[\frac{\frac{1}{J}\sum_{i=1}^{J} X_{N(i)-1}^{(i)}}{\frac{1}{J}\sum_{i=1}^{J} Y_{N(i)-1}^{(i)}}\right] - \mathrm{E}\left[\frac{\frac{1}{J}\sum_{i=1}^{J} X_0^{(i)}}{\frac{1}{J}\sum_{i=1}^{J} Y_{N(i)-1}^{(i)}}\right]
\end{aligned}$$

where A is the event

$$A = \bigcap_{i=1}^{J} \left\{ N(i) = N_i, Y_{N_i-2}^{(i)} = y_i, X_{N_i-1}^{(i)} = X_i. \right\}$$

It is difficult to tell from the analytics whether or not $\hat{\lambda}$ is biased, but we demonstrate in the Results section that $\hat{\lambda}$ underestimates λ. The variance of $\hat{\lambda}$ is given by

$$\begin{aligned}
&\mathrm{Var}\hat{\lambda} = \mathrm{Var}\left(\frac{\sum_{i=1}^{J}(Y_{N(i)}^{(i)} - X_0^{(i)})}{\sum_{i=1}^{J} Y_{N(i)-1}^{(i)}}\right) \\
&= \mathrm{Var}\left(1 + \frac{\sum_{i=1}^{J}(X_{N(i)}^{(i)} - X_0^{(i)})}{\sum_{i=1}^{J}(Y_{N(i)-2}^{(i)} + X_{N(i)-1}^{(i)})}\right) \\
&= \mathrm{Var}\left(\frac{\sum_{i=1}^{J}(X_{N(i)}^{(i)} - X_0^{(i)})}{\sum_{i=1}^{J}(Y_{N(i)-2}^{(i)} + X_{N(i)-1}^{(i)})}\right) \\
&= \mathrm{E}\left[\mathrm{Var}\left(\frac{\sum_{i=1}^{J}(X_{N(i)}^{(i)} - X_0^{(i)})}{\sum_{i=1}^{J}(Y_{N(i)-2}^{(i)} + X_{N(i)-1}^{(i)})}\,\middle|\, B(i)\right)\right] \\
&\quad + \mathrm{Var}\,\mathrm{E}\left[\frac{\sum_{i=1}^{J}(X_{N(i)}^{(i)} - X_0^{(i)})}{\sum_{i=1}^{J}(Y_{N(i)-2}^{(i)} + X_{N(i)-1}^{(i)})}\,\middle|\, B(i)\right] \\
&= \\
&\sigma^2\mathrm{E}\left[\frac{\sum_{i=1}^{J} X_{N(i)-1}^{(i)}}{\left(\sum_{i=1}^{J} Y_{N(i)-1}^{(i)}\right)^2}\right] + \mathrm{Var}\left(\frac{\sum_{i=1}^{J}(\lambda X_{N(i)-1}^{(i)} - X_0^{(i)})}{\sum_{i=1}^{J} Y_{N(i)-1}^{(i)}}\right) \\
&= \frac{\sigma^2}{J}\mathrm{E}\left[\frac{\frac{1}{J}\sum_{i=1}^{J} X_{N(i)-1}^{(i)}}{\left(\frac{1}{J}\sum_{i=1}^{J} Y_{N(i)-1}^{(i)}\right)^2}\right] \\
&\quad + \mathrm{Var}\left(\frac{\frac{1}{J}\sum_{i=1}^{J}(\lambda X_{N(i)-1}^{(i)} - X_0^{(i)})}{\frac{1}{J}\sum_{i=1}^{J} Y_{N(i)-1}^{(i)}}\right)
\end{aligned} \tag{3.5}$$

where

$$B(i) = \left(N(i), Y_{N(i)-2}^{(i)}, X_{N(i)-1}^{(i)}\right).$$

Asymptotically, as the number of runs goes to infinity, (3.5) becomes

$$\begin{aligned}
\mathrm{Var}\hat{\lambda} &\sim \frac{\sigma^2}{J}\mathrm{E}\left[\frac{\mathrm{E}\left[X_{N(i)-1}\right]}{\left(\mathrm{E}\left[Y_{N(i)-1}\right]\right)^2}\right] + \mathrm{Var}\left(\frac{\mathrm{E}\left[\lambda X_{N(i)-1} - X_0\right]}{\mathrm{E}\left[Y_{N(i)-1}\right]}\right) \\
&\sim \frac{C\sigma^2}{J},
\end{aligned}$$

where C is a constant. The standard deviation is thus proportional to $\frac{1}{\sqrt{J}}$.

3.1.2 Estimating total failures distribution

The general procedure for estimating the total failures distribution $P[Y = y]$ is

1. Assume a parameterized form for the initial failures distribution $P[X_0 = x]$ with generating function $m(s)$, and offspring distribution $P[X = x]$ with generating function $f(s)$.

2. Estimate the parameters of $m(s)$ and $f(s)$ from the data.

3. Compute the total failures distribution $P[Y = y]$ from $m(s)$ and $f(s)$ using (2.7) and (2.8)

The procedure estimates parameters of an explicit form of $m(s)$ and $f(s)$ so that the computation of $P[Y = y]$ can be done using computer algebra.

Previous work [15] has suggested that both initial line failures $P[X_0 = x]$, and offspring distribution $P[X = x]$ should be Poisson distributed. The initial distribution has mean θ, and has the form

$$P[X_0 = x] = \frac{e^{-\theta}\theta^x}{x!} \qquad r = 0, 1, 2, \ldots$$

and generating function

$$m(s) = e^{\theta(s-1)}.$$

Since cascades with zero number of failures are ignored, the initial Poisson distribution must be conditioned on nonzero failures, so

$$P[X_0 = x] = \frac{e^{-\theta}}{1 - e^{-\theta}} \frac{\theta^x}{x!} \qquad r = 1, 2, 3, \ldots. \tag{3.6}$$

Let the sample mean of the initial failures be

$$\overline{X_0} = \frac{1}{J} \sum_{i=1}^{J} X_0^{(i)}.$$

The parameter θ is then estimated by $\hat{\theta}$ by equating means:

$$\overline{X_0} = \frac{\hat{\theta}}{1 - e^{-\hat{\theta}}}.$$

If saturation effects are present in the initial stage, (3.6) may have to be altered (in some way) to include saturation. See section (4.2.4.3) for more.

The Poisson offspring distribution has form

$$P[X_0 = x] = \frac{e^{-\lambda}\lambda^x}{x!} \qquad r = 0, 1, 2, \ldots$$

and generating function

$$f(s) = e^{\lambda(s-1)}.$$

Using (2.7) and (2.8), $P[Y = y]$ is found to be a Generalized Poisson Distribution [10]. Including saturation effects S results in:

$$P[Y = y] = \begin{cases} \theta\left(y\lambda + \theta\right)^{y-1} \frac{e^{-y\lambda-\theta}}{y!}; & 0 \leq y < S \\ 1 - \sum_{i=0}^{S-1} \theta\left(i\lambda + \theta\right)^{i-1} \frac{e^{-i\lambda-\theta}}{i!}; & y = S \end{cases} \tag{3.7}$$

When conditioned on nonzero initial failures, this becomes

$$P[Y = y] = \begin{cases} \theta\left(y\lambda + \theta\right)^{y-1} \frac{e^{-y\lambda-\theta}}{y!\left(1-e^{-\theta}\right)}; & 0 \leq y < S \\ 1 - \sum_{i=0}^{S-1} \theta\left(i\lambda + \theta\right)^{i-1} \frac{e^{-i\lambda-\theta}}{i!\left(1-e^{-\theta}\right)}; & y = S \end{cases} \tag{3.8}$$

We will also make use of the "mixed" distribution

$$P[Y = y] = \begin{cases} \sum_{x=1}^{\infty} P_E[X_0 = x] \frac{x}{(y-x)!} y^{y-x-1}\lambda^{y-x}e^{-\lambda y}; & y < S \\ 1 - \sum_{j=0}^{S-1} \left(\sum_{x=1}^{\infty} P_E[X_0 = x] \frac{x}{(j-x)!} j^{j-x-1}\lambda^{j-x}e^{-\lambda j} \right); & y = S \end{cases}, \tag{3.9}$$

where

$$P_E[X_0 = x] = \frac{\sum_{k=1}^{J} 1_{X_0^k = x}(X_0^k)}{J}$$

is the observed empirical initial distribution and

$$P[Y = y | X_0 = x] = \frac{x}{(y-x)!} y^{y-x-1}\lambda^{y-x}e^{-\lambda y} \tag{3.10}$$

is the Borel-Tanner distribution. (3.10) is obtained from (2.6) when $f(s)$ is a Poisson distribution [10].

3.2 Load shed

Load shed is gathered from the simulation or system in the same format as line failures. The data must be handled in such a way that each cascade starts with a nonzero amount of shed. For example, cascades with no load shed are discarded. Again, this means that the computed pdf of load shed is conditioned on the cascade starting. Moreover, if the simulation produces some cascades with no load shed in initial stages and load shed in subsequent stages, then we choose to discard the initial stages with no load shed so that stage 0 starts with a positive amount of load shed. Then cascade i has $N(i)$ stages. $N(i)$ is determined similarly to (3.2) by either the maximum number of simulated stages being reached or the amount of load shed in a stage being zero or negligible.

3.2.1 Estimating λ and θ

λ is estimated in the same way as line failures, through use of (3.4). The mean initial load shed θ is estimated by the sample mean

$$\hat{\theta} = \frac{1}{J}\sum_{i=1}^{J} X_0^i.$$

3.2.2 Estimating blackout size pdf

The general procedure for estimating the blackout size pdf $K(x)$ is

1. Assume a parameterized form for the initial load shed cgf $m(s)$ and offspring cgf $h(s)$.
2. Estimate the parameters of $m(s)$ and $h(s)$ from the data.
3. Compute the blackout size cgf $\mathcal{K}(s)$ from $m(s)$ and $h(s)$ using (2.13) and (2.14)
4. Compute the inverse Laplace transform of $e^{-\mathcal{K}(s)}$ to obtain the blackout size pdf $K(x)$ using (2.15).

The procedure estimates parameters of an explicit form of $m(s)$ and $h(s)$ so that the computation of $\mathcal{K}(s)$ and the Laplace inversion can be done using computer algebra.

We choose to assume gamma distributions for the initial load shed and offspring distributions. Then the corresponding cgf's are

$$m(s) = \frac{\theta^2}{\sigma^2_{\text{init}}} \ln\left(1 + s\frac{\sigma^2_{\text{init}}}{\theta}\right) \tag{3.11}$$

and

$$h(s) = \frac{\lambda^2}{\sigma^2_{\text{off}}} \ln\left(1 + s\frac{\sigma^2_{\text{off}}}{\lambda}\right). \tag{3.12}$$

The parameters of the initial load shed cgf are the mean θ and the variance σ^2_{init}. The parameters of the offspring cgf are the mean λ and the variance σ^2_{off}.

The means λ and θ are estimated from the data as described in the previous subsection. The variance of the initial load shed σ^2_{init} is estimated using

$$\hat{\sigma}^2_{\text{init}} = \frac{1}{J}\sum_{i=1}^{J}(X_0^{(i)})^2 - \hat{\theta}^2.$$

The variance of the offspring distribution σ^2_{off} is estimated by applying the method of moments to X_1. The second moment of X_1 is

$$EX_1^2 = \frac{d^2}{ds^2}\, e^{-m(h(s))}\Big|_{s=0} = \lambda^2\left(\theta^2 + \sigma^2_{\text{init}}\right) + \theta\sigma^2_{\text{off}}$$

Then the estimator $\hat{\sigma}^2_{\text{off}}$ may be found by solving:

$$\frac{1}{J}\sum_{i=1}^{J}(X_1^{(i)})^2 = \hat{\lambda}^2_{\text{init}}\left(\hat{\theta}^2 + \hat{\sigma}^2_{\text{init}}\right) + \hat{\theta}\hat{\sigma}^2_{\text{off}} \tag{3.13}$$

where

$$\hat{\lambda}_{\text{init}} = \frac{1}{\hat{\theta}}\left(\frac{1}{J}\sum_{i=1}^{J} X_1^{(i)}\right).$$

3.2.3 Note on σ^2_{off} estimation

With (3.13), we estimate σ^2_{off} using only information from the X_0 and X_1 stages. This is in contrast to λ estimation where $\hat{\lambda}$ uses information from multiple stages. Ideally, we would like to find an offspring variance estimator that also uses information from all stages. One such estimator, seen in [12], is

$$\overline{\sigma}^2_{\text{off}} = \frac{1}{N}\sum_{n=1}^{N}\left(\frac{X_n}{X_{n-1}} - \hat{\lambda}\right)^2, \tag{3.14}$$

Table 3.1 Comparison of $\hat{\sigma}^2_{\text{off}}$ and $\overline{\sigma}^2_{\text{off}}$

loading factor	$\hat{\sigma}^2_{\text{off}}$	$\overline{\sigma}^2_{\text{off}}$
0.85	0.00431	0.116
0.9	0.00568	0.103
0.95	0.00995	0.130
1.0	0.01230	0.736

where

$$X_n = \sum_{i=1}^{J} X_n^i,$$

and

$$N = \max\{n | X_n > 0\}.$$

However, when we applied (3.14) to the data, it resulted in a variance estimate that seemed much too high. Also, while $\hat{\sigma}^2_{\text{off}}$ tended to increase by a factor of about 3 as the loading increased from $L = 0.85$ to $L = 1.0$, $\overline{\sigma}^2_{\text{off}}$ tended to increase by a factor of about 7. See Table 3.1 for a comparison. These results lead me to believe that $\overline{\sigma}^2_{\text{off}}$ is unsuitable for our purposes. It is not clear why this is so but one explanation could be the following: if the underlying data X_n^i does not quite describe a branching process with fixed λ, but rather a branching process with stage dependent $\lambda(n)$, then (3.14) will not work because $\left(\frac{X_n}{X_{n-1}} - \hat{\lambda}\right)^2 \to \left(\lambda(n-1) - \hat{\lambda}\right)^2 \not\to 0$ as $X_0 \to \infty$ for at least one n. Thus (3.14) will tend towards infinity. This should be the case even if the stage dependent fluctuations of $\lambda(n)$ are small.

Chapter 4

Results

This section is divided up into two parts. The first deals with the empirical statistical accuracy of the $\hat{\lambda}$ estimator. The second analyzes the results of applying the estimator on OPA simulation data.

4.1 Performance of $\hat{\lambda}$ on Monte Carlo

The $\hat{\lambda}$ was first tested on a sequence of discrete state branching processes, with $X_0 = 1$ and Poisson offspring distribution, generated by Monte Carlo. The estimator mean $\mu(\hat{\lambda})$ and standard deviation $\sigma(\hat{\lambda})$ were recorded. First, various numbers $10 \leq J \leq 1000$ of cascades were generated with saturation $S = 20$, and for various offspring means $0 < \lambda < 2$. The simulation was run for 10 stages. $\hat{\lambda}$ was found to underestimate λ with a bias of less that 0.1:

$$-0.1 \leq \mu(\hat{\lambda}) - \lambda < 0.$$

The bias tended to decrease as more cascades J are considered for statistics. As predicted, the standard deviation $\sigma(\hat{\lambda})$ was seen to decrease as roughly

$$\sigma(\hat{\lambda}) \leq \frac{0.6}{\sqrt{J}}$$

as J increases.

The process was repeated for saturation $S = 100$. Increasing the saturation had the effect of improving the performance of $\hat{\lambda}$ as it allows more information to be included. Here

$$-.07 \leq \mu(\hat{\lambda}) - \lambda < 0.$$

and

$$\sigma(\hat{\lambda}) \leq \frac{0.5}{\sqrt{J}}$$

$\hat{\lambda}$ was also tested on continuous state branching processes, with $X_0 = 1$ and Gamma offspring distribution. Various numbers $10 \leq J \leq 1000$ of cascades were generated for various offspring means $0 < \lambda < 2$. The offspring variance was varied throughout the range $0 < \sigma^2_{\text{off}} < \lambda^2$, where $\sigma^2_{\text{off}} = \lambda^2$ is the exponential distribution. Saturation was not considered. The simulation was run for 10 stages. $\hat{\lambda}$ was found to underestimate λ with a bias of less than 0.06:

$$-0.06 \leq \mu(\hat{\lambda}) - \lambda < 0.$$

The bias tended to decrease as more cascades J are considered for statistics. The standard deviation $\sigma(\hat{\lambda})$ was seen to decrease as roughly

$$\sigma(\hat{\lambda}) < \frac{0.45}{\sqrt{J}}$$

as J increases.

4.2 Estimating $\hat{\lambda}$ and blackout distributions on OPA model

The estimated propagation $\hat{\lambda}$ and total cascade sizes are estimated on data produced by the OPA power system using the methods described in Section 3.

4.2.1 OPA model operation

The OPA power system simulation produces cascading transmission line outages and load shed in stages resulting from an initial disturbance. It accepts input files specifying the configuration of buses and lines, as well as system characteristics such as load profile, line ratings, and generator capacity. The initial disturbance is produced either by forcing a random number of lines to trip, by overloading the system to the point where some lines reach their MW limits, or by a combination of the two. The initial disturbance causes the system to redispatch generation and/or shed load via a DC load flow optimal LP dispatch algorithm. This may cause

more lines to trip, and system redispatches again. This trip/dispatch procedure is allowed to continue several times to represent a cascading blackout. The simulation outputs two sets of numbers for each trial run: a sequence of line failures representing the line failure cascade and a sequence of load shed representing the load shed cascade. The simulation is repeated until sufficient cascades are produced for statistical analysis. [6] contains a detailed description of OPA.

The input file we used was the IEEE 118 system, with load profile shown in Section 7.3. The OPA parameters were $\gamma = 1.67$, $p_0 = 0.0001$, $p_1 = 1.0$. The small probability p_0 of forced line trips signifies that the cascades we produced were mostly due to overloading. The loading level L is the multiplier applied to the base load profile that determines the initial loading of the system. We varied L and inspected its effect on the statistics. The loadings we chose were $L = 0.85, 0.9, 0.95, 1.0, 1.3$.

4.2.2 Data Preparation

In order to prepare the OPA cascades to match the form (3.1), a number of preprocessing steps needed to be taken. First, any stage of a cascade with load shed $< 10^{-15}$ is set to zero. This is because the OPA simplex solver sometimes erroneously gives a small negative load shed instead of a small positive one for orders lower than this. I would suggest that this means that load shed below this order is inaccurate. Load shed is measured as a fraction of total system demand, meaning the maximum shed is 1, or total blackout. In real systems, the load shed will not be accurate to within the level of 10^{-15}, in fact it will probably only be measured to a couple of significant figures. (Under these circumstances the mathematics of section (2.2) may need to be altered to include conditioning on $X_n \geq \rho$, where ρ is the minimum level of precision.)

The second preprocessing step is to discard any cascade of zero failures or zero load shed. It should be noted that the line failures and load shed parts are decoupled so that discarding any line failure cascade does not necesarily mean discarding the load shed cascade and vice versa. Additionally any initial stages of zero load shed must be discarded so that each cascade

begins with nonzero shed. The simulation produces 10 stages including the initial stage, so after preprocessing each cascade will have a length up to $N(i) = 9$.

The third step is to set saturation for line failures and to set aside line failure cascades that saturate in the first two stages ($Y_1 \geq S$) when computing (3.4), since by the definition of (3.4) these cannot be used.

We wished to apply our estimators to a set of $J = 5000$ nontrivial OPA cascades for each loading level L. So enough cascades were generated so that after preprocessing, $J = 5000$ cascades were used for both load shed and line outages. This is sufficent to ascertain λ to within a reasonable accuracy as well as construct probability distribution functions of total failures and load shed.

4.2.3 $\hat{\lambda}$ results

Table 4.1 displays the estimated propagation at each load level, with line outages and load shed displayed side by side. Saturation was set to $S = 15$ for line failures and ignored for load shed. We assume that saturation effects for load shed are minimal for subcritical λ. This may or may not be the case, but we currently have no way of including saturation into the load shed framework so it is a necessary assumption. There are no visible humps in the load shed pdfs for subcritical cases that would suggest saturation. Results for $L \geq 1$ are not available for load shed because we are not yet able to deal with the saturation effects that seem to be present in this regime. Also, another caveat is that the $S = 15$ setting for line failures is largely a guess.

$\hat{\lambda}$ is seen to increase as L increases, which is intuitive since a higher stressed system should have higher propagation. Also, the two sets of $\hat{\lambda}$ match up quite well. This match tends to support the assertion that a single λ determines the cascading process of both line failures and load shed.

4.2.4 Cascade size distributions

Table 4.2 shows all the initial and offspring parameters estimated from the data that are needed to construct the distributions $P[Y = y]$ for line failures and $K(x)$ for load shed.

Table 4.1 Estimated propagation $\hat{\lambda}$ from load shed and line outage data

loading factor	load shed $\hat{\lambda}$	line outages $\hat{\lambda}$
0.85	0.128	0.115
0.9	0.159	0.188
0.95	0.264	0.288
1.0	0.429	0.430

4.2.4.1 Line failures distributions

After pdfs were constructed from the data set, we produced estimates of the pdfs using the methods of Section 3. Figure 4.1 compares the estimated and empirical distributions of total line failures Y for loading level $L = 0.85$. This is repeated for loading levels $L = 1$ and $L = 1.3$ in Figures 4.2 and 4.3 respectively. The total failures are plotted on a log-log scale over two decades, from a single line failure to 100 line failures. (There are 179 lines in the network total.) The Generalized Poisson Distribution (3.8) is used with $S = 15$ for the estimated fit. Additionally, the "mixed fit" of (3.9) is used with $S = 15$. The fits for $L = 0.85$ and $L = 1$ seem to work fairly well. Figure 4.3 ($L = 1.3$) is an interesting case, and is discussed in Section 4.2.4.3.

4.2.4.2 Note on Saturation

In figures 4.2 and 4.3, there are no empirical data points past saturation $S = 15$, because we have modified the empirical distribution by moving all probability mass $Y \geq S$ to the hypothesized saturation point $S = 15$ as described in Section 2.2.1. To see the empirical pdfs without this modification, see Figures 4.4, and 4.5. Figure 4.1 shows no change as there were no cascades reaching $S = 15$ for $L = 0.85$.

4.2.4.3 Discussion of Figure 4.3

In Figure 4.3, the fit of (3.8) does not match up with the fit using an empirical initial distribution. The mixed fit does not fit well either, and in fact fits worse than that of (3.8) which

Table 4.2 Estimated initial line outages, initial load shed and load shed offspring distribution parameters

loading factor	load shed $\hat{\lambda}$	line outages $\hat{\lambda}$	load shed $\hat{\theta}$	line outages $\hat{\theta}$	$\hat{\sigma}^2_{\text{init}}$	$\hat{\sigma}^2_{\text{off}}$
0.85	0.128	0.115	0.0520	0.985	0.00198	0.00431
0.9	0.159	0.188	0.0482	1.088	0.00195	0.00568
0.95	0.264	0.288	0.0445	1.325	0.00182	0.00995
1.0	0.429	0.430	0.0383	1.628	0.00160	0.01230
1.3	n/a	0.570	n/a	12.296	n/a	n/a

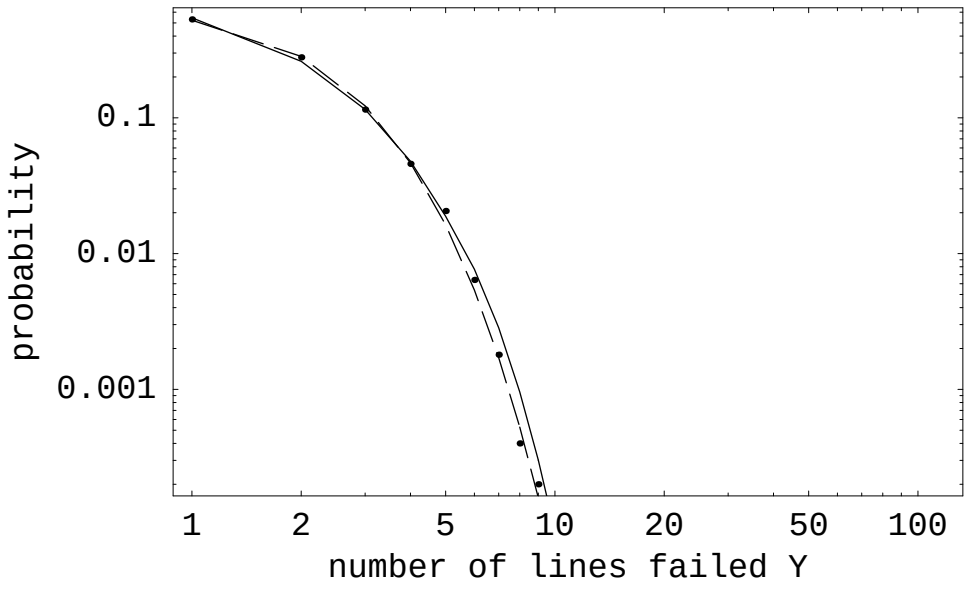

Figure 4.1 Probability distribution of total line failures Y on log-log scale. Empirical distribution shown as dots, estimated distribution with (3.8) shown as dashed line, estimated distribution with empirical initial failures (3.9) shown as solid line. Empirical pdf unmodified. IEEE 118 bus system with loading $L = 0.85$.

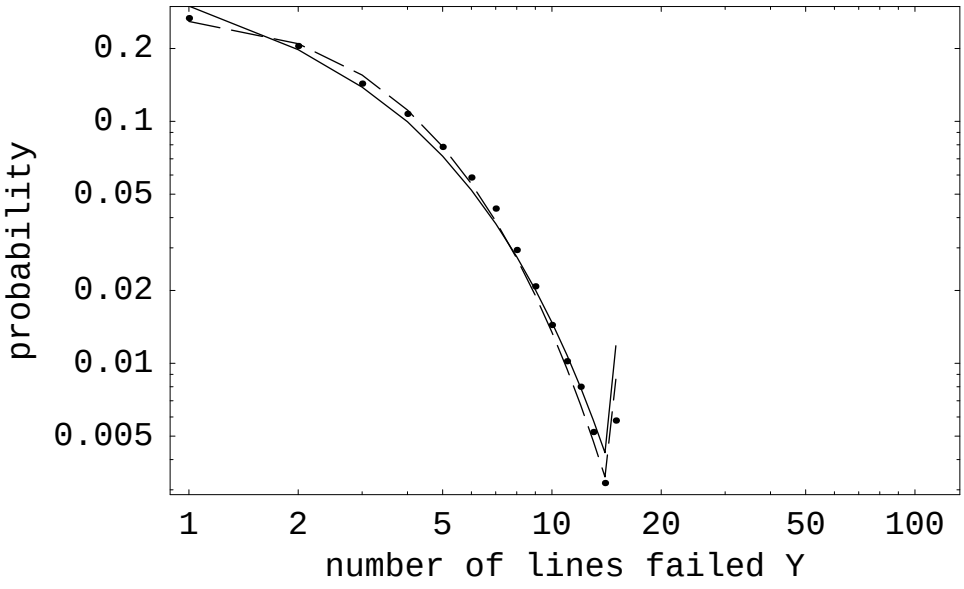

Figure 4.2 Probability distribution of total line failures Y on log-log scale. Empirical distribution shown as dots, estimated distribution with (3.8) shown as dashed line, estimated distribution with empirical initial failures (3.9) shown as solid line. Empirical pdf modified. IEEE 118 bus system with loading $L = 1.0$.

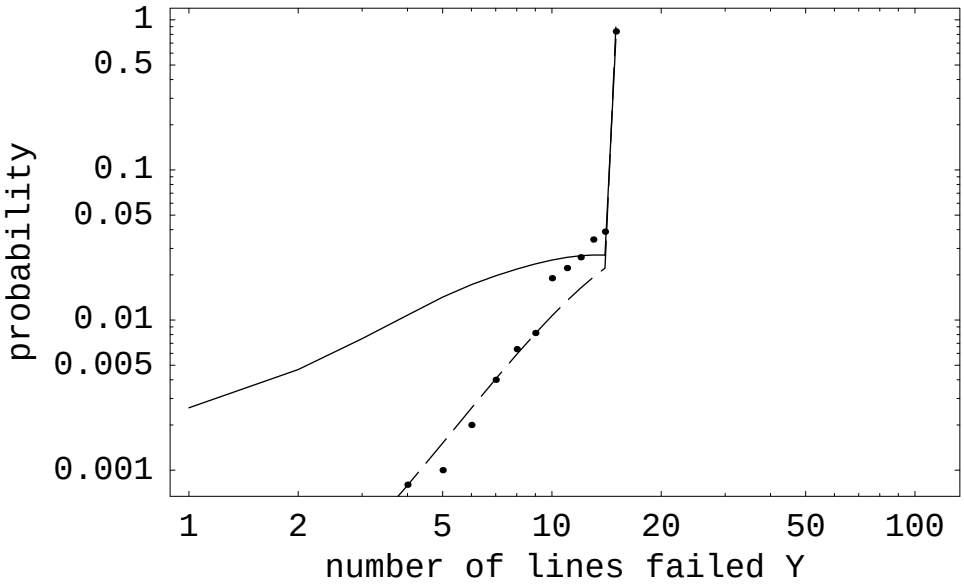

Figure 4.3 Probability distribution of total line failures Y on log-log scale. Empirical distribution shown as dots, estimated distribution with (3.8) shown as dashed line, estimated distribution with empirical initial failures (3.9) shown as solid line. Empirical pdf modified. IEEE 118 bus system with loading $L = 1.3$.

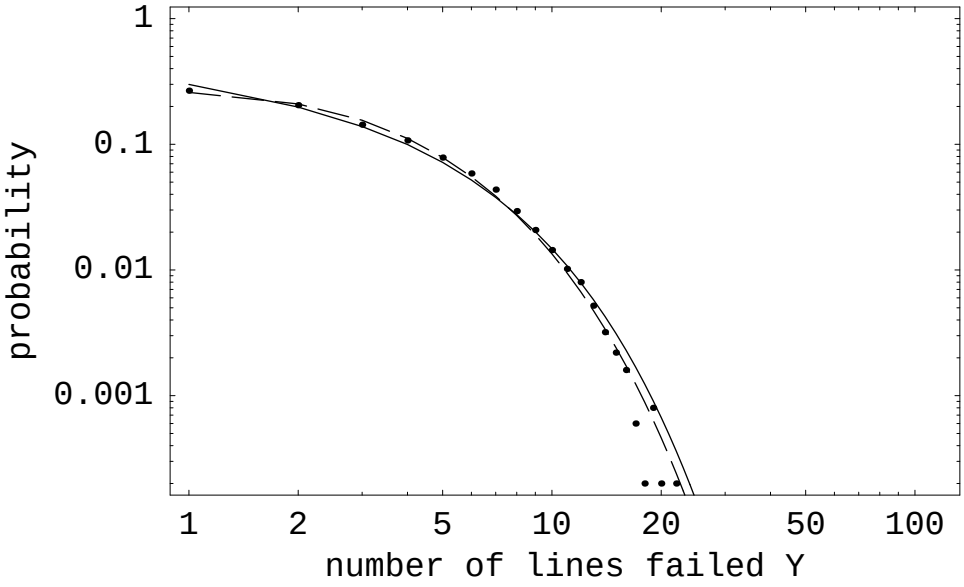

Figure 4.4 Probability distribution of total line failures Y on log-log scale. Empirical distribution shown as dots, estimated distribution with (3.8) shown as dashed line, estimated distribution with empirical initial failures (3.9) shown as solid line. Empirical pdf unmodified. IEEE 118 bus system with loading $L = 1.0$.

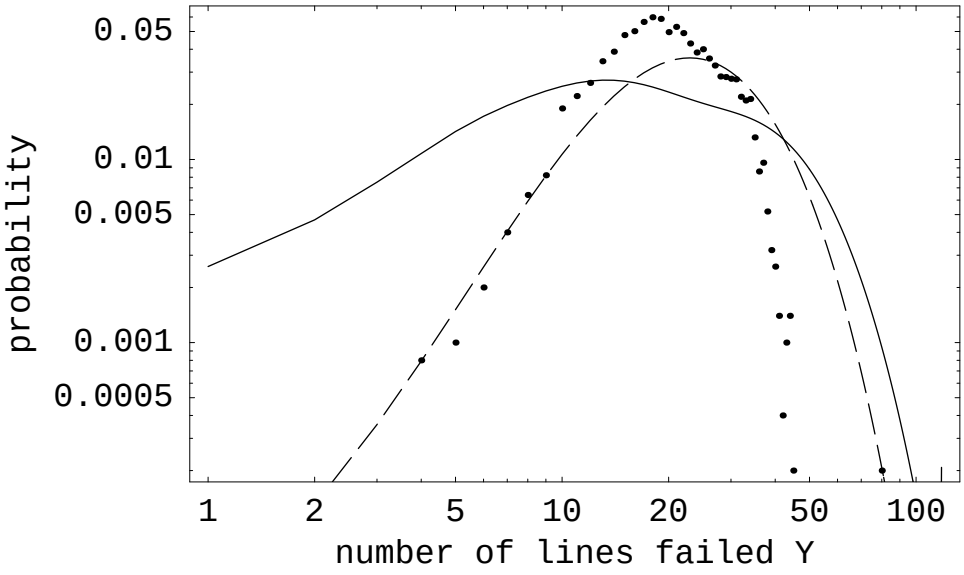

Figure 4.5 Probability distribution of total line failures Y on log-log scale. Empirical distribution shown as dots, estimated distribution with (3.8) shown as dashed line, estimated distribution with empirical initial failures (3.9) shown as solid line. Empirical pdf unmodified. IEEE 118 bus system with loading $L = 1.3$.

is counterintuitive. I believe the poor fits are related the fact that, at this high loading level, many of the cascades saturate immediately at the initial stage. This can be seen by looking at the plot of the initial failures distribution (Figure 4.6). To properly deal with initial saturation, (3.6) and θ estimation would have to be altered to include saturation effects, although it is not yet clear how to do so. One idea is to remove runs for which $X_0 \geq S$ from θ estimation and ignore these runs when performing estimation of θ. The result in this case is the initial distribution fit shown in Figure 4.7 and the total failures distribution shown in Figure 4.8. Two effects can be observed: the initial fit in Figure 4.7 is better, and the mixed of Figure 4.8 matches up better with the fit using (3.8). However, the total failures empirical distribution still does not match the fits.

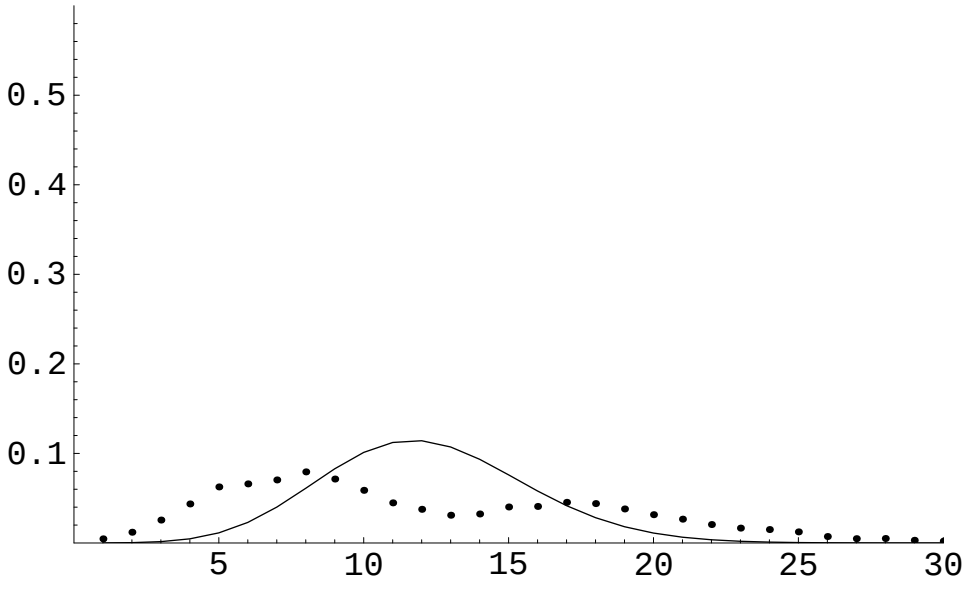

Figure 4.6 Probability distribution of initial line failures X_0 for $L = 1.3$. Empirical is dots, Poisson is solid. $\hat{\theta} = 12.206$

4.2.4.4 Load shed distributions

Figure 4.9 compares the empirical and estimated pdfs for loading level $L = 0.85$, and Figure 4.11 compares the empirical and estimated pdfs for loading level $L = 1.0$. The blackout size is plotted on a log scale over two decades, from a small blackout $Y = .01$ (shedding of 1%

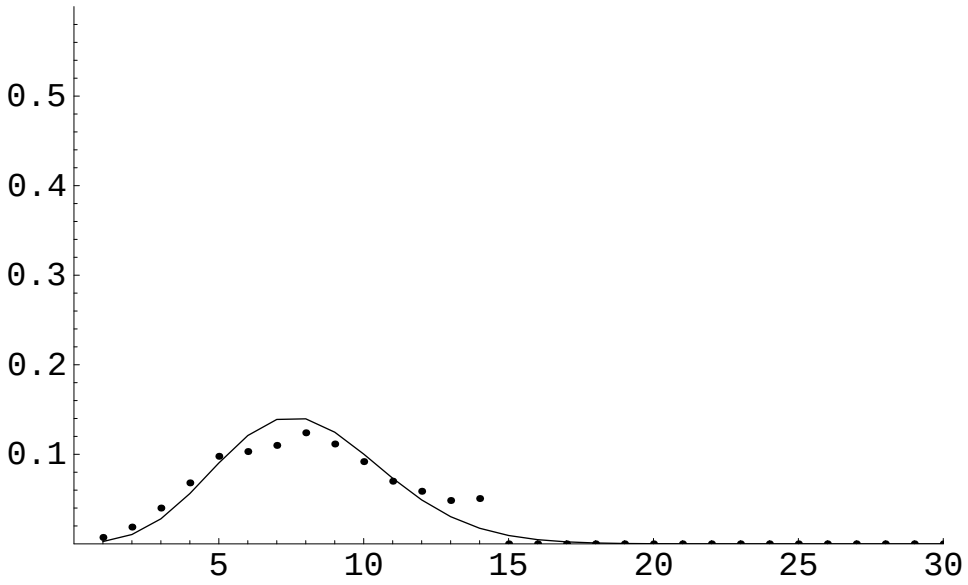

Figure 4.7 Probability distribution of initial line failures X_0 for $L = 1.3$. Empirical is dots, Poisson is solid. OPA runs with $X_0 \geq 15$ removed. $\hat{\theta} = 8.039$

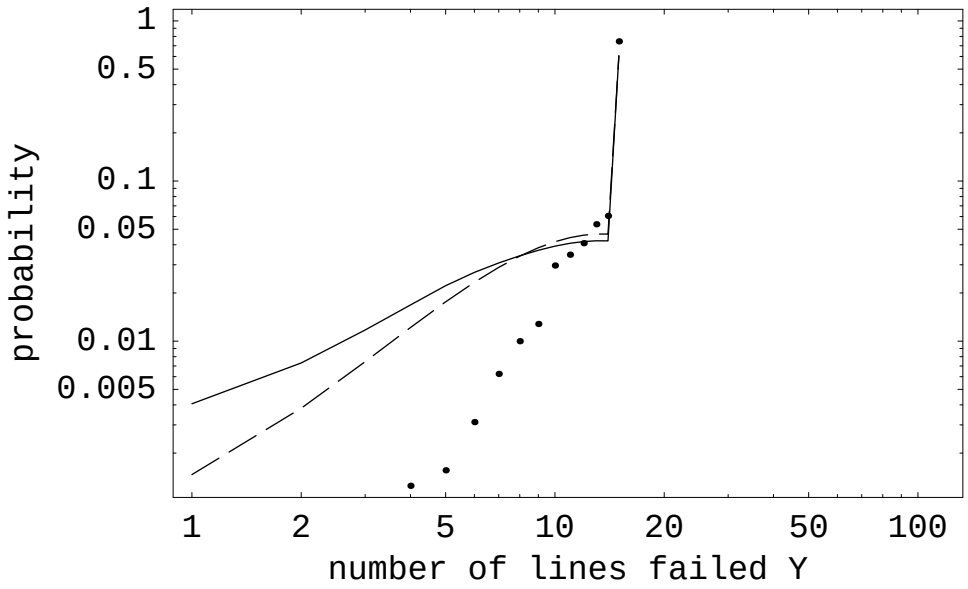

Figure 4.8 Probability distribution of total line failures Y on log-log scale for $L = 1.3$. Empirical is dots, GPD is dashed, mixed is solid. OPA runs with $X_0 \geq 15$ removed. Empirical pdf modified.

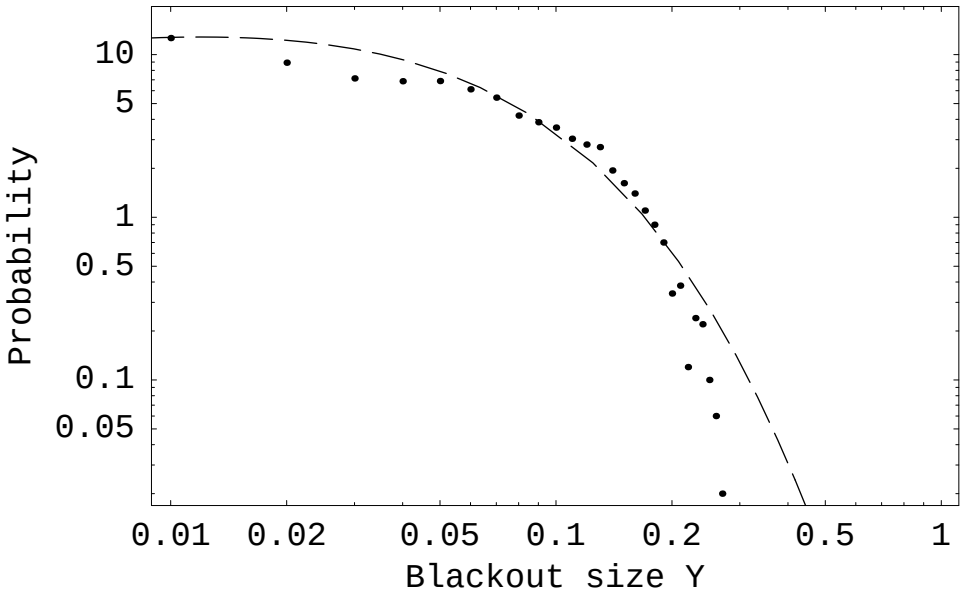

Figure 4.9 Probability density function of blackout size Y on log-log plot. Empirical pdf shown as dots, estimated pdf shown as dashed line. IEEE 118 bus system with loading $L = 0.85$.

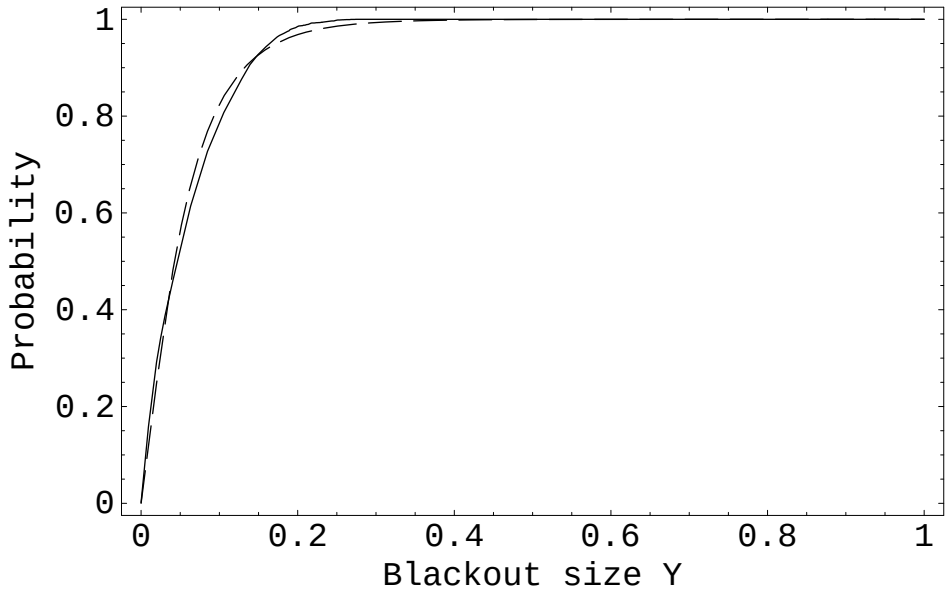

Figure 4.10 Cumulative distribution function of blackout size Y. Empirical cdf shown as solid line, estimated cdf shown as dashed line. IEEE 118 bus system with loading $L = 0.85$.

of total load) to $Y = 1$ (shedding of 100% of total load and total blackout). The corresponding cgfs are also plotted in Figure 4.10 and Figure 4.12 to give another view of how well the empirical and estimated distributions match.

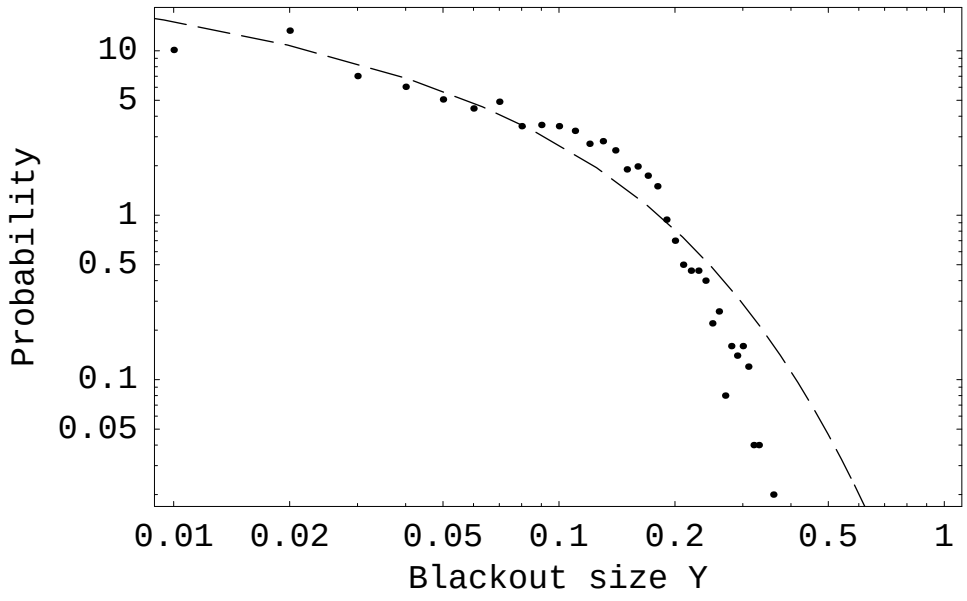

Figure 4.11 Probability density function of blackout size Y on log-log plot. Empirical pdf shown as dots, estimated pdf shown as dashed line. IEEE 118 bus system with loading $L = 1.0$.

4.2.4.5 Initial load shed and offspring distribution

We discuss the choices of the forms of initial load shed and offspring distributions that are assumed in the computations.

The initial load shed gamma distribution parameters $\hat{\theta}$ and $\hat{\sigma}^2_{init}$ shown in Table 2 are relatively insensitive to loading changes. For all these cases $\hat{\sigma}^2_{init} \approx \hat{\theta}^2$ and hence the initial load shed is approximately exponentially distributed. Figure 4.13 shows estimated and empirical initial failure distributions for loading $L = 1.0$.

Figure 4.14 shows the estimated offspring distribution pdf for loading $L = 1.0$. This is a gamma distribution with mean 0.0383 and variance 0.00160 that is approximately a normal distribution. However, the offspring pdf becomes more asymmetrical when the loading L is

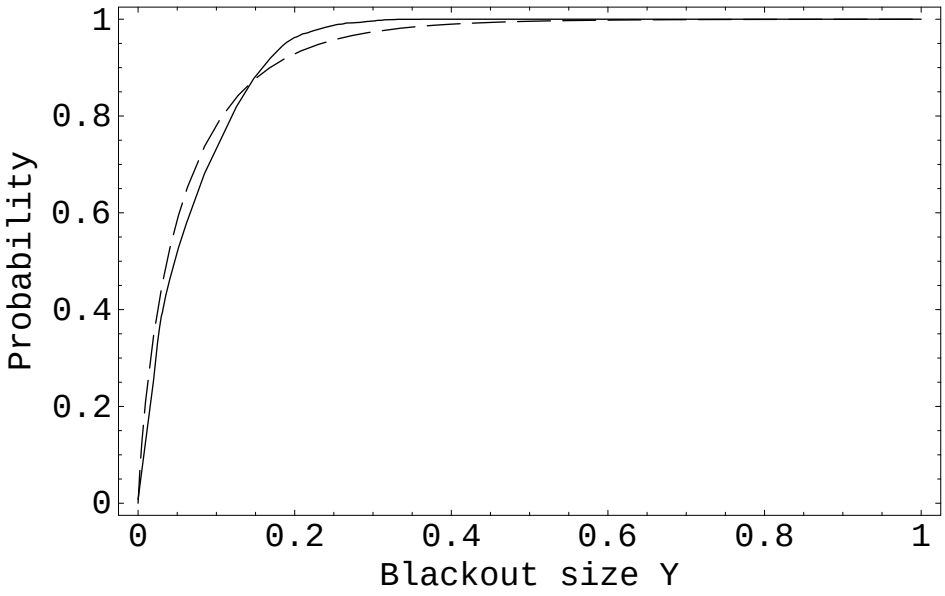

Figure 4.12 Cumulative distribution function of blackout size Y. Empirical cdf shown as solid line, estimated cdf shown as dashed line. IEEE 118 bus system with loading $L = 1.0$.

decreased. Any parameterized nonnegative distribution that is infinitely divisible is a candidate to describe the offspring distribution and we have not found general arguments supporting our specific choice of the gamma distribution.

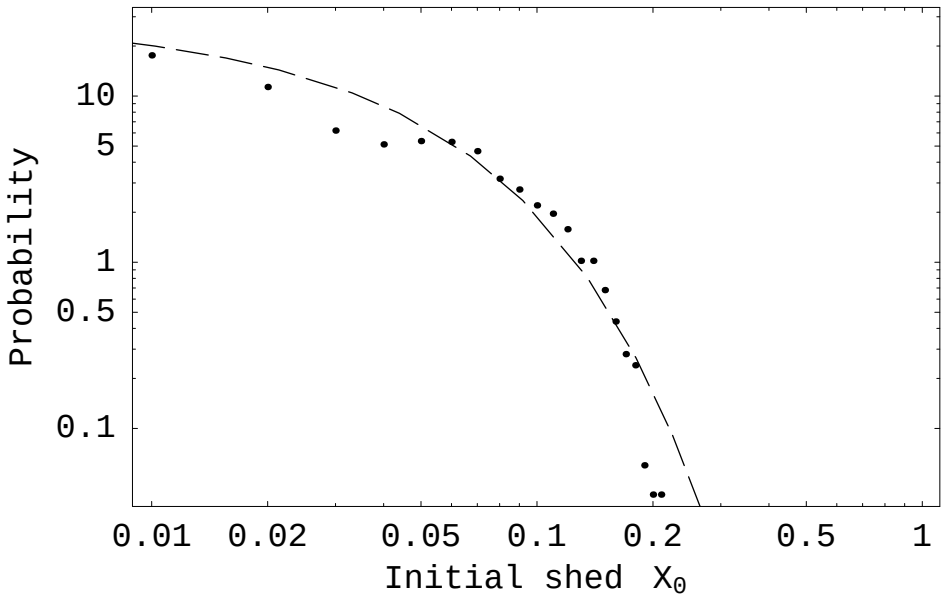

Figure 4.13 Probability density function of initial load shed X_1 on log-log plot. Empirical pdf shown as dots, estimated pdf shown as dashed line. IEEE 118 bus system with loading $L = 1.0$.

4.2.5 Influencing λ

The main method we used to influence $\hat{\lambda}$ in OPA was to raise or lower the loading factor L. As seen in Table 4.1, increasing L caused λ to increase. It can also be seen in Table 4.1 that we had a difficult time trying to push OPA to criticality, where $\lambda = 1$. For line outages, increasing L had a much more significant effect on θ. An approximate 10-fold increase in θ was accompanied by only an approximate doubling of λ. (For load shed, a different effect was observed; θ did not change appreciably as L was increased). We then tried a number of alterations to the OPA model in hopes that we could obtain a critical or supercritical response. The alterations were:

1. Decrease the loading factor L while increasing p_0

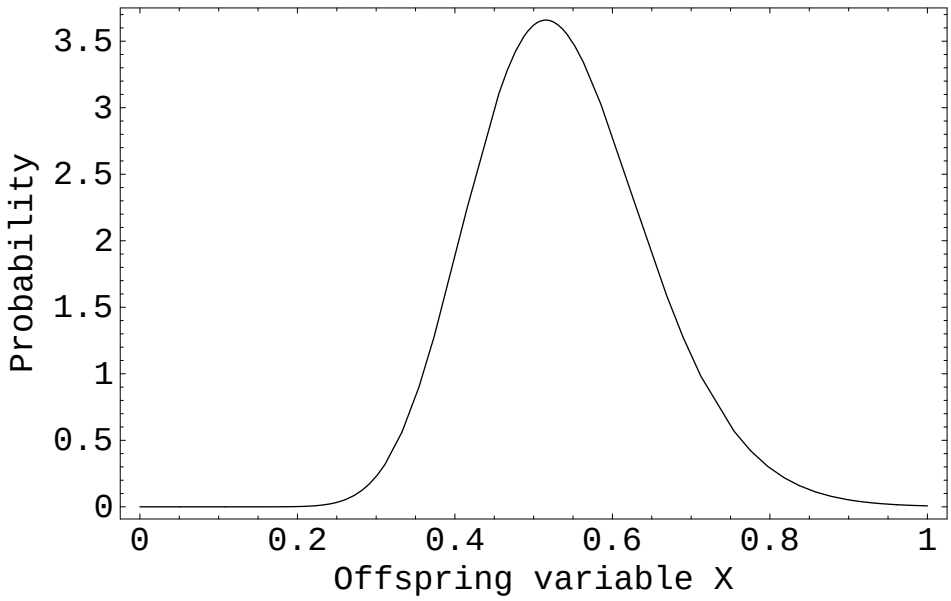

Figure 4.14 Probability density function $H(x)$ of offspring distribution that is a gamma distribution with mean $\lambda = .429$ and variance $\sigma^2_{\text{off}} = .0123$. Parameters computed from data on IEEE 118 bus system with loading $L = 1.0$.

2. Decrease load fluctuations γ while increasing L

3. Increase the individual line limits.

None of these, however, had the effect of increasing $\hat{\lambda}$ near 1.

Chapter 5

Miscellaneous Topics

5.1 Correction in [24]

We found Theorem 2.2 in Guttorp's *Statistical Inference for Branching Processes* to be incorrect. The theorem reads:
For fixed n as $z \to \infty$:

1. if $m < \infty$, $\hat{m}_n(z) \to m$ a.s. and $\mathrm{E}\hat{m}_n(z) \to m$
2. if $\sigma^2 < \infty$, then

$$\left(\frac{z}{\sigma^2} \frac{(m-1)^2}{\sum_0^{2n} m^i - (2n+1)m^n} \right)^{1/2} (\hat{m}_n(z) - m) \xrightarrow{d} \mathrm{N}(0,1),$$

where it should read
For fixed n as $z \to \infty$:

1. if $m < \infty$, $\hat{m}_n(z) \to m$ a.s. and $\mathrm{E}\hat{m}_n(z) \to m$
2. if $\sigma^2 < \infty$, then

$$\left(\frac{z}{\sigma^2} \frac{m-1}{m^n - 1} \right)^{1/2} (\hat{m}_n(z) - m) \xrightarrow{d} \mathrm{N}(0,1),$$

as shown in [48, 11]. This has been verified by Monte Carlo simulation.

5.2 Critical Infrastructure Paper

I contributed to the research and writing of [3], which demonstrated simple DC load flow algorithms that can be used to analyze the effect of terrorist attacks on a power grid.

5.3 Discrete Map Interpretation of Branching Processes

The stagewise cumulative offspring generating function, F_n, of a Galton Watson branching process is definied iteratively: $F_{n+1}(s) = sf(F_n(s))$. Its most interesting feature is that when certain conditions are met, this iterative procedure converges to a generating function with power law expansion of index $-3/2$, independent of specific details of f. I interpret this iterative procedure as a two-dimensional discrete map, and show that it contains a tangent (saddle node) bifurcation. It then follows, from the work of others, that this map displays scaling relations and power law sensitivity to initial conditions in certain regions. The resulting scaling exponents are universal, independent of the specific form of f and an index of 3/2 can even be recovered (although its relation to the power law expansion of F is not clear)

5.3.1 Branching Process Recap

I'm assuming knowledge of branching processes so I will just state some relevant results as found in [26]. The offspring generating function is $f(s) = \sum_{n=0}^{\infty} p_n s^n$ and has mean $f^{'}(1) = \lambda$. The cumulative progeny generating function at stage n is $F_n(s) = \sum_{n=1}^{\infty} P_n s^n$ and is defined by

$$F_{n+1}(s) = sf(F_n(s)). \tag{5.1}$$

As $n \to \infty$, $F_n(s)$ converges to the total progeny generating function $F(s)$ as defined by

$$F(s) = sf(F(s)).$$

I will focus on the set $\mathcal{F}$ of $f(s)$ when f satisfies the conditions $\lambda = 1$,$p_0 > 0$, and $p_0 + p_1 < 1$. When these conditions hold, the expansion of $F(s)$ goes as [31]

$$P_n = \begin{cases} q\left(\frac{1}{2\pi f''(1)}\right)^{1/2} n^{-3/2} + O(n^{-5/2}) & n = 1 \bmod q; \\ 0 & n \neq 1 \bmod q \end{cases}, \tag{5.2}$$

where q is the largest integer such that $p_n \neq 0$ implies that q divides n. The radius of convergence of this power series is 1.

I will need a sample $f(s)$ for examples; the Poisson generating function $f_p(s) = e^{\lambda(s-1)}$ will be used for that purpose. It can be verified that $f_p \in \mathcal{F}$.

5.3.2 Discrete Map Formulation

I now introduce the two-dimensional discrete map M:

$$x_{n+1} = x_n \tag{5.3}$$

$$y_{n+1} = x_n f(y_n), \tag{5.4}$$

subject to the constraints $x_n\, y_n > 0$. This puts the iterative nature of $F(s)$ on a dynamical systems/discrete map footing. F can now be analyzed using discrete iterative map terminology and techniques. The motivation is to find any scaling exponents of F and determine if any any are equal to $-3/2$, the exponent of (5.2). So, looking at M, note first that the trajectories only move in the y direction. Note also that when the initial condition (x_0, y_0) is such that $x_0 = y_0$, the y_n component of the trajectory $\{(x_0, y_0), (x_1, y_1), (x_1, y_1), \ldots\}$ corresponds to the sequence $\{F_1(y_0), F_2(y_0), F_3(y_0), \ldots\}$. So $F(s)$ is the attracting set of all points that start on the line $s = x_0 = y_0$. To further explore the properties of M we must only notice that any vertical "cross section" of fixed $x_n = c$, leads to the reduced map

$$y_{n+1} = cf(y_n),$$

so we can deduce the properties of the vertical strips by looking at graphs of s vs $cf(s)$. When $0 < c < 1$, there are two fixed points, one stable and one unstable, where the stable point is equal to $F(c)$. When $c > 1$, There are no fixed points, and all trajectories diverge towards $y_\infty = \infty$. The most interesting behavior of M is when $c = 1$. Here

$$y_{n+1} = f(y_n) \tag{5.5}$$

describes a tangent bifurcation since $f'(1) = \lambda = 1$. The fixed point is approached by points on the vertical line $L = \{1\} \times (0, 1)$. Also, this fixed point $(1, 1)$, now called z_{tb}, corresponds to $F(1) = 1$.

To display other properties of M, I generated the phase space plot Figure 5.4 using the example offspring generating function $f_P(s)$.

S denotes the attracting set of points while U denotes the unstable set of fixed points. All were found by running sample trajectories forwards and backwards in "time." The point z_{tb}

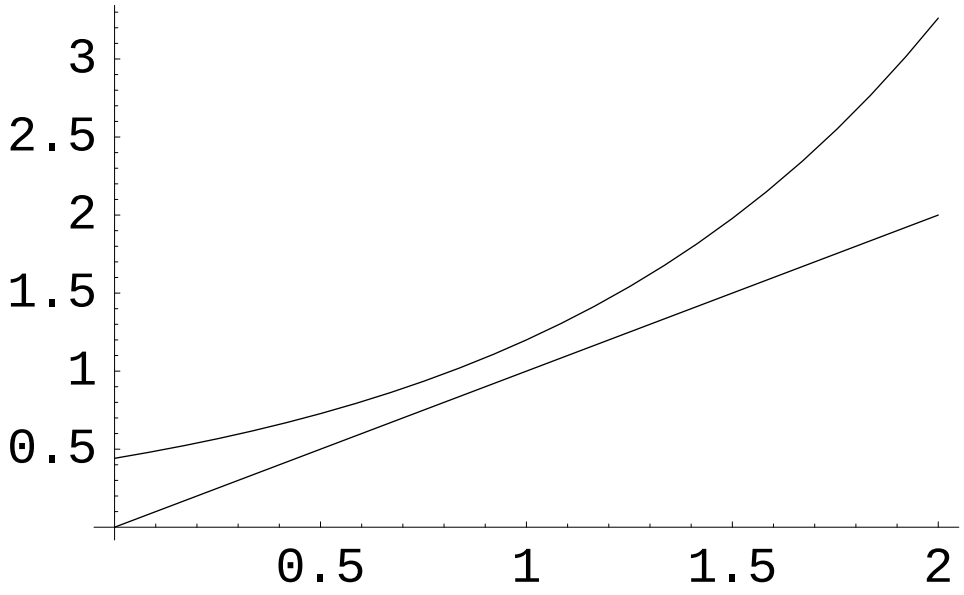

Figure 5.1 Graph of $1.2f_p(s)$ displaying no fixed points

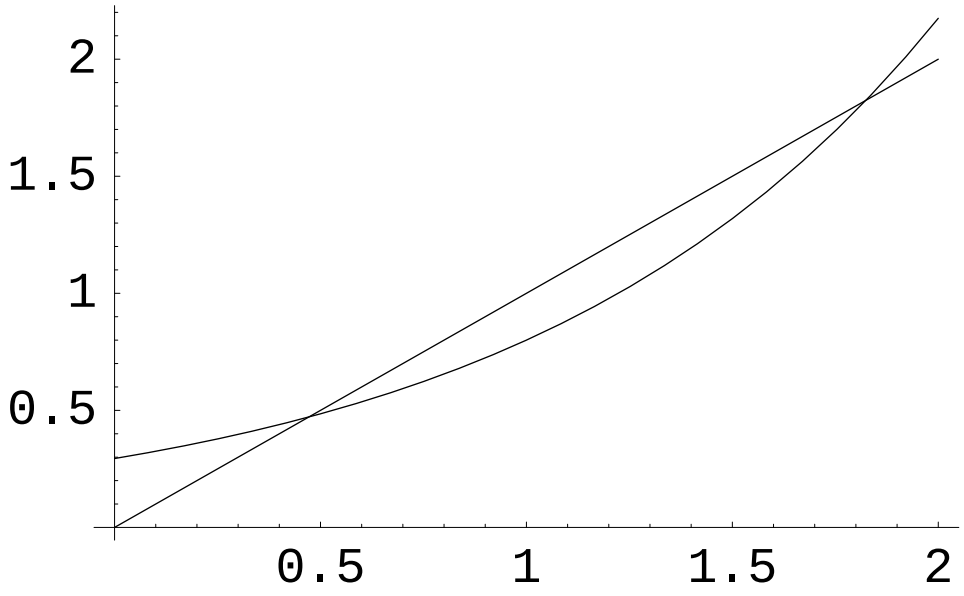

Figure 5.2 Graph of $.8f_p(s)$ displaying one stable and one unstable fixed points

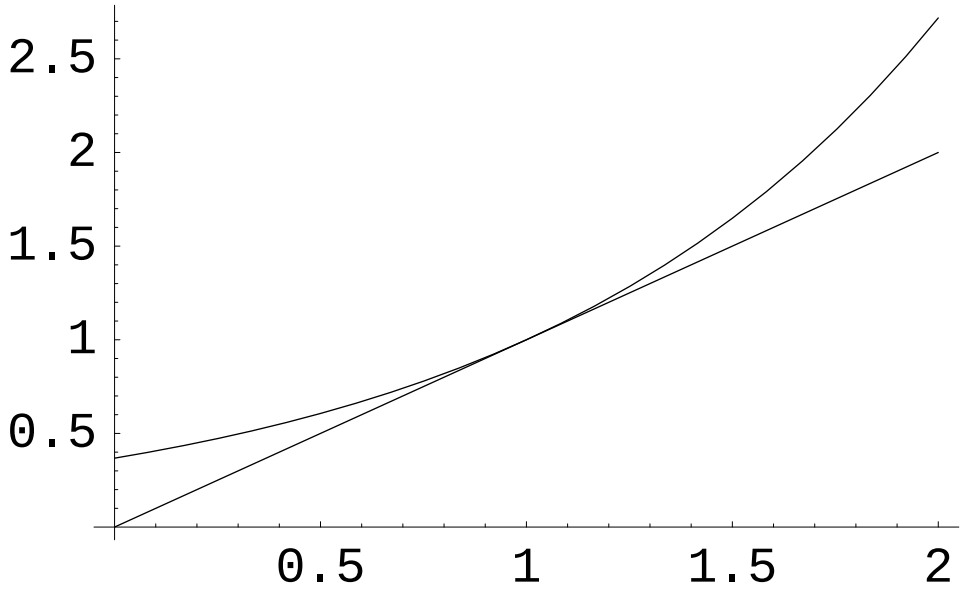

Figure 5.3 Graph of $f_p(s)$ displaying the tangent bifurcation at $(s, f(s)) = (1, 1)$

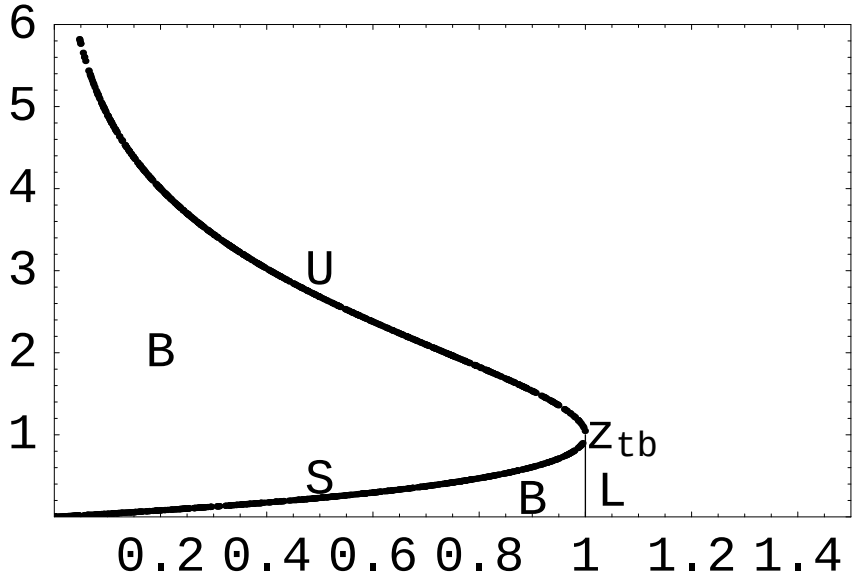

Figure 5.4 First quadrant phase space of $f_p(s)$ displaying the set of stable fixed points S, set of unstable fixed points U, critical point z_{tb}, basin of attraction B, and critical region L.

joins both sets. Now that the attracting set has been found, convergence properties can be explored. Sample paths are chosen close to the attractor and lyapunov exponents computed by the method in [37]. Clearly there is exponential convergence of nearby trajectories for initial points chosen in $(0,1) \times (0,u)$, where $u \in U$. The interesting behavior is for trajectories on L. These, which converge to z_{tb} have lyapnuov exponent of zero and thus display sub-exponential convergence/divergence of nearby trajectories. It has been suggested [33] that there is a power-law convergence of nearby trajectories (power-law insensitivity to initial conditions) here which I explain later. The basin of attraction, B, is then described by all points in $(0,1) \times (0,u)$ where $u \in U$, those that converge exponentially to S. The strip $L = \{1\} \times (0,1)$ is the set that converges, subexponentially to the point$(1,1)$. The set $\overline{B \bigcup L \bigcup U}$ is the set that diverges to infinity. These qualitative properties are universal for $f \in \mathcal{F}$.

The result of this is that investigation of scaling properties of M reduces to investigation of scaling properties of (5.5), the one dimensional discrete map at tangent bifurcation.

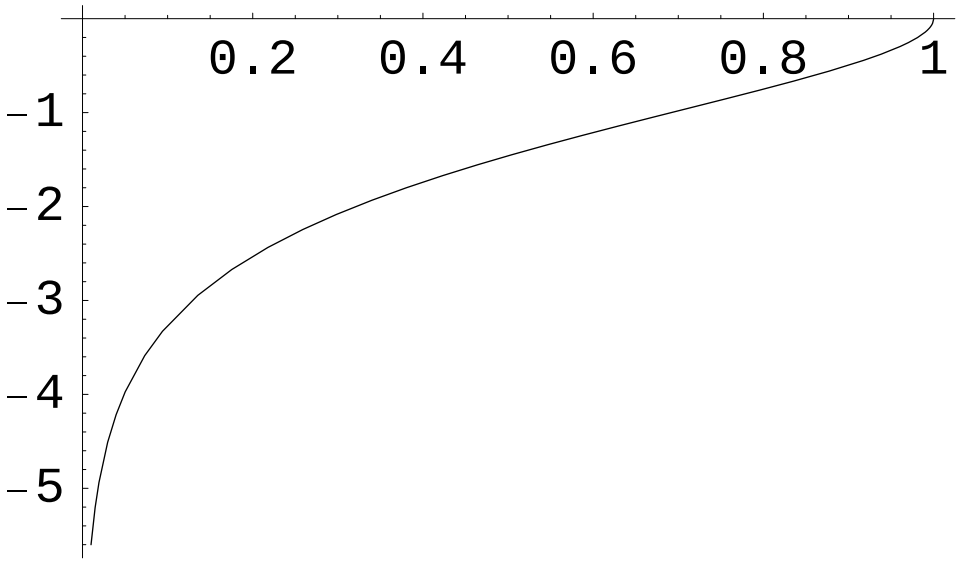

Figure 5.5 Graph of lyapunov exponent versus x_n coordinate for points in B. The lyapunov exponent is zero at $x_n = 1$

5.3.3 Scaling Properties

I now restrict attention to the "interesting" part of the phase space: the section $L = \{1\} \times (0, 1)$ where trajectories converge to z_{tb}. Dropping the x_n component and shifting the map so that z_{tb} is at $y_n = 0$ results in the map:

$$y_{n+1} = g(y_n), \tag{5.6}$$

where

$$g(s) = f(s + 1) - 1.$$

This defines a one-to-one correspondence between the set $f \in \mathcal{F}$ and a new set $g \in \mathcal{G}$.

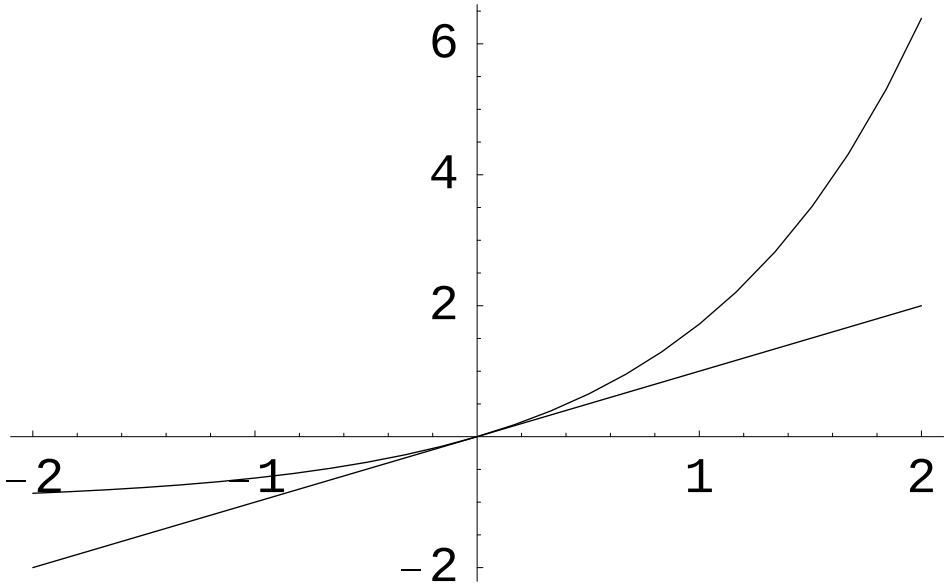

Figure 5.6 Graph of $g_p(s)$ displaying the tangent bifurcation at $(s, g(s)) = (0, 0)$

Now consider the set $\mathcal{Q}$ which is the subset of $\mathcal{G}$ for which $g^{'}(0) = 1$, $g \in \mathcal{G}$. $q \in \mathcal{Q}$ can be written

$$q(s) = s + us^z + O(s^{z+1})$$

. It has been shown [27] that $q(s)$ converges under repeated applications of the rescaling operator

$$T[q(s)] = \alpha q(q(\frac{1}{\alpha}s))$$

(in the region about the origin) to the map

$$q^*(s) = s\left(1-(z-1)us^{(z-1)}\right)^{-1/(z-1)}$$

which displays the Feigenbaum scaling property [20],[21],[27]

$$q^*(q^*(s)) = q^{*2}(s) = \frac{1}{\alpha}q^*(\alpha s). \tag{5.7}$$

The value of α is given by $\alpha = 2^{1/(z-1)}$ where z signifies the "universality class" of the map and is the index of the second lowest order term in the expansion $q(s) = s + us^z + O(s^{z+1})$. Note that $q^*(s)$ also has expansion $q^*(s) = s + us^z + O(s^{z+1})$ around zero. Also, when $s_0 < 0$, $q^n(s_0)$ converges under functional iteration to $q^{*n}(s)$.

The map $g(s)$ is, as shown in Section 5.3.6, always of universality class $z = 2$, so $\alpha = 2$, and thus the scaling relation for the fixed point $g^*(s)$ is

$$g^*(g^*(s)) = g^{*2}(s) = \frac{1}{2}g^*(2s).$$

Also, the exact solution of (5.7) is

$$g^*(s) = \frac{s}{1-us},$$

and when $y_0 < 0$,

$$g^n(y_0) \to g^{*n}(y_0). \tag{5.8}$$

See Section 5.3.6 for convergence proofs.

5.3.4 Power Laws: Convergence and Sensitivity to Initial Conditions

A convenient approximation can be made after noticing (5.8) as well as the property

$$\begin{aligned} g^{*n}(y_0) &= \frac{1}{n}\left(g^*(ny_0)\right) \\ &= \frac{1}{n}\left(\frac{ny_0}{1-uny_0}\right) \\ &= \frac{y_0}{1-uny_0}, \end{aligned} \tag{5.9}$$

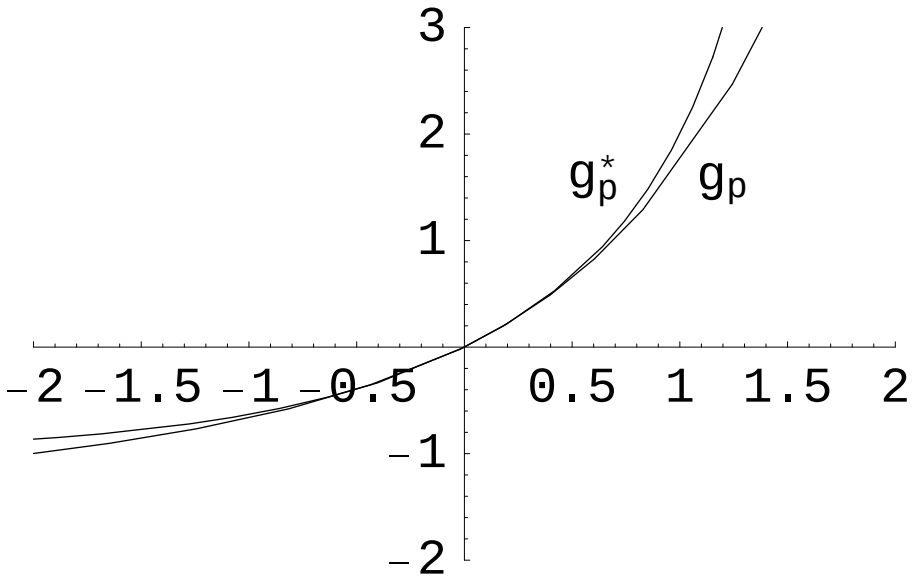

Figure 5.7 The map $g_P(s) = f_p(s+1) - 1$ converges under rescaling T to $g_P^*(s)$ in the region about the origin

where (5.9) can be easily verified by induction. Now the discrete time map can be imagined, as in [33], as a continuous time flow

$$g_t(y_0) = \frac{y_0}{1 - uty_0}. \tag{5.10}$$

In fact, this is the solution to the vector field equation

$$\dot{x} = ux^2, \tag{5.11}$$

so the study of M and (5.6) has been further reduced to the study of a one-dimensional vector field at a tangent bifurcation. The solution (5.10) shows that for large t, i.e. as the flow approaches the origin,

$$g_t(y_0) \approx (-ut)^{-1},$$

so the trajectory has a limiting power law form of exponent 1. Translating back to f should result in

$$f_t(y_0) \approx 1 + (-ut)^{-1},$$

and simulation appears to support it (below).

Also, a sensitivity to initial conditions can be computed from the continuous time flow by considering (using notation from [33])

$$\xi_t(y_0) = \frac{dg_t(y_0)}{dy_0} = \frac{1}{(1 - uty_0)^2}. \tag{5.12}$$

When t is large, this takes the power law form

$$\xi_t(y_0) \approx (uty_0)^{-2},$$

with exponent -2. Again, simulation seems to support this result.

In [33], it is claimed that the exponent $3/2$ can be recovered by interpreting (5.12) in terms of a "q-generalized" lyapunov exponent λ_q, where

$$\xi_t(y_0) = \exp_q(\lambda_q t) \equiv (1 - (q-1)\lambda_q t)^{-1/(q-1)}. \tag{5.13}$$

This function has interesting properties and plays a central role in Tsallis non-extensive statistical mechanics [41], a new theory of statistical mechanics that can be used to derive both

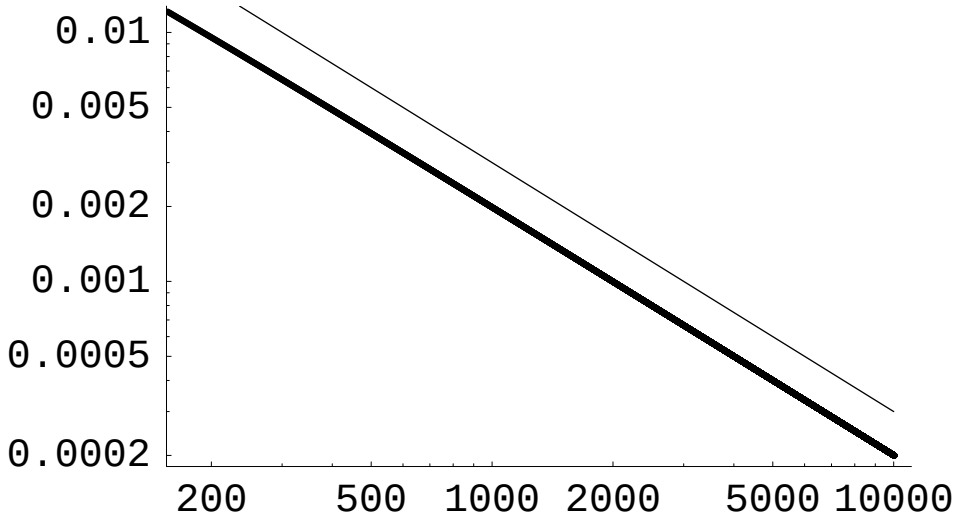

Figure 5.8 Log-Log plot of $f_P^n(.8)$ vs. iteration number n (lower) and a power law of index -1 (upper)

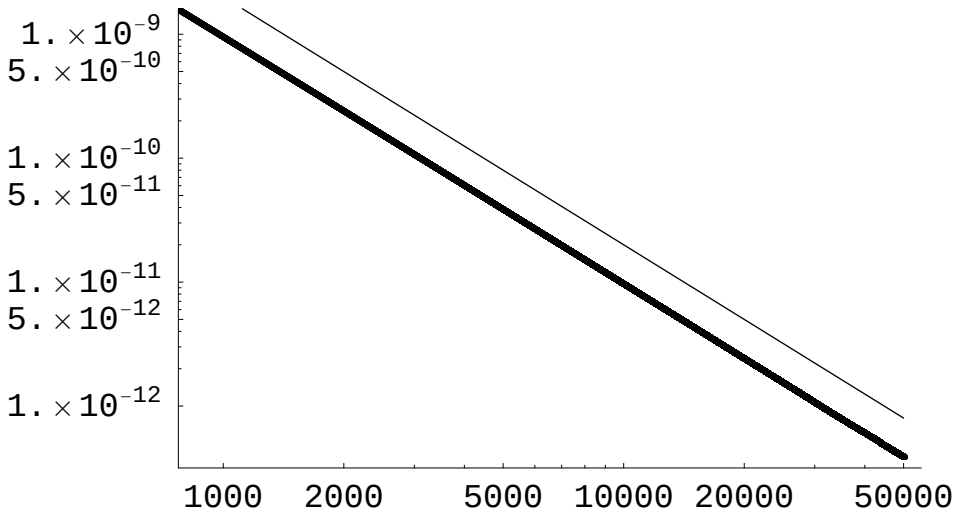

Figure 5.9 Log-Log plot of $f_P^n(.8) - f_P^n(.80001)$ vs iteration number n (lower) and a power law of index -2 (upper)

exponential distributions (as in traditional statistical mechanics) and power law distributions. However, it is a fairly contentious theory at the moment (see [23]), so I will merely state its existence. Notice that (5.12) and (5.13) are equivalent when $q = 3/2$ and $\lambda_q = 2uy_0$. It is not clear how this may be connected to the $-3/2$ exponent of (5.2). I'll also note that [40] recovers a power law exponent of near $3/2$ using a box counting method. Again any connection is unclear.

5.3.5 Conclusion

By recasting (5.1) as a map M (5.3),(5.4), the total progeny generating function $F(s)$ can be seen as the attractor S of M. Then any power law properties of (5.1) seem highly correlated with power law properties of the convergence to S. This reduces to the study of scaling exponents of a one-dimensional map (5.5) or flow (5.11) at a tangent bifurcation. The flow (5.11) converges to its fixed point with exponent -1 and displays insensitivity to initial conditions with exponent -2. Using the statistical mechanics concepts of [41], this insensitivity to initial conditions can be written as a q-exponential of index $3/2$. Further research would have to investigate the nature of the q-exponential and any relationship to (5.2).

5.3.6 Appendix for Discrete Map Interpretation of Branching Process

5.3.6.1 A1: Equivalence class for $\mathcal{G}$

I will show that an arbitrary g in $\mathcal{G}$ has expansion $g(s) = s + us^2 + O(s^3)$. Any g is equivalent to an $f(s)$ in $\mathcal{F}$ shifted so that the point of tangency is at the origin:

$$\begin{aligned} g(s) &= f(s+1) - 1 \\ &= -1 + p_0 + p_1(s+1) + p_2(s+1)^2 + p_3(s+1)^3 \ldots \\ &= -1 + \sum_{n=0}^{\infty} p_n + \sum_{n=1}^{\infty} n p_n s + \sum_{n=2}^{\infty} \binom{n}{2} p_n s^2 + O(s^3) \\ &= s + us^2 + O(s^3), \end{aligned}$$

where $u = \sum_{n=2}^{\infty} \begin{pmatrix} n \\ 2 \end{pmatrix} p_n$. This result follows from the fact that $\sum_{n=0}^{\infty} p_0 = f(1) = 1$ and $\sum_{n=1}^{\infty} np_n = f^{'}(1) = \lambda = 1$

5.3.6.2 A2: Demonstration of convergence to $g^*(s)$

Write $g(s)$ as

$$g(s) = g^*(s) + h(s),$$

where $h(s)$ has leading term of order s^n, $n > 2$. Restrict attention to the region about the origin. Now

$$\begin{aligned} g^2(s) &= g^* \left((g^*(s) + h(s)) + h \left(g^*(s) + h(s) \right) \right. && (5.14) \\ &\approx g^{*2}(s) + g^{*'}(g^*(s))h(s) + h(g^*(s)) + h^{'}(g^*(s))h(s) && (5.15) \\ &\approx \frac{1}{2} g^*(2s) + g^{*'}(g^*(s))h(s) + h(g^*(s)) + h^{'}(g^*(s))h(s). && (5.16) \end{aligned}$$

To consider eigenfunctions, solutions of the form

$$g^2(s) = \frac{1}{2} g^*(2s) + \frac{\lambda}{2} h_\lambda(2s) \tag{5.17}$$

are needed. Combining (5.16) and (5.17), the eigenfunction equation becomes

$$g^{*'}(g^*(s))h_\lambda(s) + h_\lambda(g^*(s)) + h_\lambda^{'}(g^*(s))h_\lambda(s) = \frac{\lambda}{2} h_\lambda(2s).$$

Expanding this and equating powers leads to the eigenvalues $\lambda_n = 4/2^n$ when h_λ has leading term s^n, $n > 2$. The fact that $|\lambda_n| < 1$ shows that since $g(s)$ and $g^*(s)$ only differ in the terms of order greater or equal to x^3,

$$\begin{aligned} g^2(s) &= \frac{1}{2} g^*(2s) + \frac{\lambda}{2} h_\lambda(2s) \\ g^4(s) &= \frac{1}{4} g^*(4s) + \frac{\lambda^2}{4} h_\lambda(4s) \\ g^{2^m}(s) &= \frac{1}{2^m} g^*(2^m s) + \frac{\lambda^{2^{m-1}}}{2^m} h_\lambda(2^m s), \end{aligned}$$

so it can be said that, using (5.9),

$$g^m(s) \rightarrow \frac{1}{m} g^*(ms) \tag{5.18}$$

$$\rightarrow g^{*m}(s) \tag{5.19}$$

and since

$$T^m(g(s)) = 2^m g^{2^m}(\frac{1}{2^m} s),$$

it follows that

$$T^m(g(s)) \rightarrow g^*(s)$$

by (5.19).

Chapter 6

Conclusions and Future Work

In this thesis we have introduced a way to use branching processes to model simulated power system cascades of failures. We can estimate the propagation parameter λ and construct probability distributions for line failures and load shed. The parameter λ is the offspring mean of the branching process model. $\lambda < 1$ means that the cascade dies out on average as it progresses in time, while $\lambda > 1$ means that the cascade grows on average. A power system simulation of $\lambda > 1$ would be expected to produce many cascading failures and a large blackout.

We have tested our methods on the OPA power system simulation. Our results for λ show that we have been operating OPA in a subcritical regime ($\lambda < 1$). Also, the λ estimates for line failures match up well with the λ estimates for load shed, suggesting that a single λ may be used to gauge both cascades in question. If this is the case, we can estimate the propagation of load shed by monitoring the progagation of line outages and vice versa. This would reduce the amount of data needed for estimation. Our estimated distributions show a reasonable similarity to the empirical distributions generated by OPA. Future work would have to quantify the similarity by way of Kolmogorov-Smirnov tests or similar methods. We have shown that estimating distributions with branching processes is fairly efficient, since only tens of cascades are needed to estimate λ to within 0.1.

Future work would apply these methods to other power system simulations, such as those found in [25, 29]. Eventually, if the method becomes sufficiently established in simulated blackouts, it may be applied to real blackout data. A number of issues would have to be

addressed in the meantime, such as improving the modeling of saturation and applying it to load shed. Also, more efficient estimators may be found such as an improved estimate for σ^2_{off}.

Efficient estimation of λ and blackout size distributions using limited data could be used in a number of important ways. System planners could use our methods on model systems to evaluate the risk of system upgrades. Extension of our methods to real power systems would enable system operators to monitor blackout risk from modest amounts of historical data. In both cases the branching process approximation of cascading failure greatly simplifies the modeling and reduces the amount of data needed to analyze risk. Branching processes also have served as a way of representing cascading failure of other complex interconnected systems. Modeling power system blackouts this way draws helpful analogies to other fields. This project is both a first step toward the goals of efficent blackout risk analysis and improving the understanding of cascading blackouts of power transmission systems.

Chapter 7

Appendix

7.1 Lagrange Inversion

We use the Lagrange Inversion technique to to approximate the cumulant generating function for continuous state branching processes. It can also be used to solve for the probability generating function for discrete state branching processes.

7.1.1 Lagrange Inversion Theorm

Let $\phi(z)$ be a function analytic on and inside the contour C surrounding a point s, and let t be such that the inequality

$$|t\phi(z)| < |z - s| \tag{7.1}$$

is satisfied at all points z on the perimeter of C; then the equation

$$\zeta = s + t\phi(\zeta), \tag{7.2}$$

regarded as an equation in ζ, has one root in the interior of C; and further ζ can be expanded as a power series

$$\zeta = s + \sum_{a=1}^{\infty} \frac{t^a}{a!} \frac{d^{a-1}}{dz^{a-1}} \left(\phi(z)^a\right)\Big|_{z=s}. \tag{7.3}$$

This method is called Lagrange Inversion. This uses the definition and language found in [45].

7.1.2 Continuous State Branching Process

In Section 2.2, the total load shed cumulant generating function $k(s)$ is given implicitly by (2.12):

$$k(s) = s + h(k(s)) \tag{7.4}$$

for $s \in \{0, \infty\}$. This is equivalent to (7.2) when $t = 1$ and $h(z) \equiv \phi(z)$. Thus (7.3) can be used given that for each $s \in \{0, \infty\}$, a contour C in the positive half-plane surrounding s can be found that satisfies

$$|h(z)| < |z - s|$$

on the edge of C. If we define the function

$$\psi(z) = |z - s| - |h(z)|, \tag{7.5}$$

then condition (7.1) is equivalent to requiring $\psi(z) > 0$ on C. Kallenburg [28] shows that $h(z)$ is analytic on the positive half-plane and concave on $z \in \{0, \infty\}$. He [28] also shows that when $\lambda < 1$, then $h(z) < z$ on $z \in \{0, \infty\}$. $k - h(k)$ is then increasing on $k \in \{0, \infty\}$ and vanishes for $k = 0$ so a unique solution can be found for any $s \in \{0, \infty\}$. It remains to be proven that the contour C exists for suitable ranges of λ and σ^2_{off}.

7.1.3 Discrete State Branching Process

The Lagrange inversion method can be used in a similar sense to solve for the generating function for discrete state branching processes. The inversion method has been used previously for this purpose in [26, 31, 10].

7.2 Laplace Inversion: Post-Widder method

Let $g(x)$ be a smooth function defined on $\mathcal{R}^{\geq 0}$. The Laplace transform of $g(x)$ is

$$G(s) = \int_0^\infty e^{-sx} g(x) dx.$$

The Post-Widder inversion method [46] gives $g(x)$ as:

$$g(x) = \lim_{a \to \infty} \frac{(-1)^a}{a!} \left(\frac{a}{s}\right)^{a+1} G^{(a)}\left(\frac{a}{s}\right), \tag{7.6}$$

where G^a is the ath derivative of $G(s)$. For this thesis, we evaluate (7.6) at finite a rather than take the limit, to gain an approximation of $g(x)$. In [42] it is shown that when $g(x) \in L_2\left(\mathcal{R}^{\geq 0}\right)$ is twice differentiable with $x^2 \frac{d^2 g(x)}{dx^2} \in L_2\left(\mathcal{R}^{\geq 0}\right)$, this approximation converges to $g(x)$ at a rate of order $O\left(\frac{1}{a}\right)$:

$$\left\| \frac{(-1)^a}{a!} \left(\frac{a}{s}\right)^{a+1} G^{(a)}\left(\frac{a}{s}\right) - g(x) \right\|_{L_2\left(\mathcal{R}^{\geq 0}\right)} \leq \frac{C}{a}, \tag{7.7}$$

where the constant C depends on the function $g(x)$. Examples below estimate C for relevant distributions of mean λ and variance σ^2. C was estimated by numerically computing the left hand side of (7.7) for various a.

1. Approximation of exponential distribution with $\lambda = .5$, $\sigma^2 = 0.25$ has $C \approx 0.35$
2. Approximation of gamma distribution with $\lambda = .5$, $\sigma^2 = .05$ has $C \approx 2.50$
3. Approximation of gamma distribution with $\lambda = .5$, $\sigma^2 = .40$ has $C \approx 0.26$
4. Approximation of gamma distribution with $\sigma^2 \geq 2\lambda^2$ does not converge in L_2 since $g(x) \notin L_2\left(\mathcal{R}^{\geq 0}\right)$.

The accuracy of the Post Widder method is highly dependent on the distribution used. It is difficult to estimate C for a typical total load shed distribution $K(x)$, (2.15), since an analytic expression for the distribution is unavailable. I hypothesize that using $a = 15$ terms gives "reasonable" accuracy, and this seems to be true after visually comparing the results with Monte Carlo generated $K(x)$. Also, since determination of $K(x)$ often requires use of a Lagrange inversion approximation, it is possible that both these forms of approximation can interact to produce error. Before fitting data to a pdf $K(x)$ using a_1 term Lagrange approximation and a a_2 Laplace approximation, I think it's a good idea to compare $K(x)$ against a Monte Carlo generated pdf to test accuracy. The accuracy will likely depend on the parameters λ, θ, σ^2_{off}, and σ^2_{init}.

7.3 OPA load profile

Here is the OPA input file used in Section 4.2:

$1 -6810.48 0 0 a0 (80, 15) [1, 2]

$1 -2670.78 0 0 a1 (99, 31) [0, 11]

$1 -5208.01 0 0 a2 (72, 33) [0, 4, 11]

$3 -5208.01 0 26336.8 a3 (54, 63) [4, 10]

$1 -1602.47 0 0 a4 (64, 83) [2, 3, 5, 7, 10]

$1 -6944.02 0 0 a5 (79, 89) [4, 6]

$1 -2537.24 0 0 a6 (87, 99) [5, 11]

$3 -3739.08 0 26131.9 a7 (64, 91) [4, 8, 29]

$1 -1602.47 0 0 a8 (46, 163) [7, 9]

$2 0 0 5.85 a9 (22, 239) [8]

$1 -9347.73 0 0 a10 (88, 59) [3, 4, 11, 12]

$3 -6276.33 0 22120.8 a11 (120, 59) [1, 2, 6, 10, 13, 15, 116]

$1 -4540.32 0 0 a12 (143, 70) [10, 14]

$1 -1869.55 0 0 a13 (147, 74) [11, 14]

$1 -12018.5 0 0 a14 (166, 84) [12, 13, 16, 18, 32]

$1 -3338.47 0 0 a15 (134, 89) [11, 16]

$1 -1468.93 0 0 a16 (146, 110) [14, 15, 17, 29, 30, 112]

$1 -8012.33 0 0 a17 (170, 106) [16, 18]

$1 -6009.25 0 0 a18 (185, 101) [14, 17, 19, 33]

$1 -2403.7 0 0 a19 (176, 133) [18, 20]

$1 -1869.55 0 0 a20 (175, 163) [19, 21]

$1 -1335.39 0 0 a21 (188, 195) [20, 22]

$1 -934.773 0 0 a22 (184, 213) [21, 23, 24, 31]

$3 -1736.01 0 26538.6 a23 (227, 213) [22, 69, 71]

$2 0 0 23536.3 a24 (182, 251) [22, 25, 26]

$2 0 0 23962.5 a25 (184, 265) [24, 29]

$3 -9481.29 23385.3 23385.3 a26 (95, 224) [24, 27, 31, 114]

$1 -2270.16 0 0 a27 (85, 191) [26, 28]

$1 -3204.93 0 0 a28 (92, 166) [27, 30]

$1 -1602.47 0 0 a29 (149, 126) [7, 16, 25, 37]

$3 -5742.17 0 23155.9 a30 (107, 169) [16, 28, 31]

$1 -7878.79 0 0 a31 (120, 192) [22, 26, 30, 112, 113]

$1 -3071.39 0 0 a32 (196, 92) [14, 36]

$1 -7878.79 0 0 a33 (218, 102) [18, 35, 36, 42]

$1 -4406.78 0 0 a34 (207, 128) [35, 36]

$1 -4139.7 0 0 a35 (224, 129) [33, 34]

$1 -1602.47 0 0 b36 (241, 94) [32, 33, 34, 37, 38, 39]

$1 -1602.47 0 0 b37 (241, 94) [29, 36, 64]

$1 -3605.55 0 0 a38 (256, 75) [36, 39]

$3 -8813.56 0 26654.6 b39 (269, 65) [36, 38, 40, 41]

$1 -4940.94 0 0 b40 (284, 65) [39, 41]

$3 -12819.8 0 24334.3 b41 (322, 65) [39, 40, 48]

$1 -2403.7 0 0 b42 (270, 119) [33, 43]

$1 -2136.62 0 0 b43 (305, 104) [42, 44]

$1 -7077.56 0 0 b44 (305, 124) [43, 45, 48]

$3 -3739.08 0 24262.1 b45 (285, 161) [44, 46, 47]

$1 -4540.32 0 0 b46 (319, 150) [45, 48, 68]

$1 -2670.78 0 0 b47 (337, 133) [45, 48]

$3 -11617.8 23841.6 23841.6 b48 (358, 144) [41, 44, 46, 47, 49, 50, 53, 65, 68]

$1 -2270.16 0 0 b49 (286, 124) [48, 56]

$1 -2270.16 0 0 b50 (395, 120) [48, 51, 57]

$1 -2403.7 0 0 b51 (352, 92) [50, 52]

$1 -3071.39 0 0 b52 (353, 69) [51, 53]

$3 -15089.9 26200.7 26200.7 b53 (385, 68) [48, 52, 54, 55, 58]

$1 -8412.95 0 0 b54 (453, 59) [53, 55, 58]

$1 -11217.3 0 0 b55 (427, 68) [53, 54, 56, 57, 58]

$1 -1602.47 0 0 b56 (408, 94) [49, 55]

$1 -1602.47 0 0 b57 (411, 97) [50, 55]

$3 -36990.3 0 29704.1 b58 (521, 125) [53, 54, 55, 59, 60, 62]

$1 -10416 0 0 b59 (523, 171) [58, 60, 61]

$2 0 29554.8 29554.8 b60 (520, 188) [58, 59, 61, 63]

$1 -10282.5 0 0 b61 (512, 206) [59, 60, 65, 66]

$1 -1602.47 0 0 b62 (514, 128) [58, 63]

$1 -1602.47 0 0 b63 (512, 181) [60, 62, 64]

$2 0 32366.7 32366.7 b64 (383, 182) [37, 63, 65, 67]

$3 -5208.01 25086.6 25086.6 b65 (387, 169) [48, 61, 64, 66]

$1 -3739.08 0 0 b66 (429, 164) [61, 65]

$1 -1602.47 0 0 b67 (350, 207) [64, 68, 80, 115]

$2 0 29626.4 29626.4 b68 (335, 209) [46, 48, 67, 69, 74, 76]

$1 -8813.56 0 0 b69 (280, 233) [23, 68, 70, 73, 74]

$1 -1602.47 0 0 b70 (270, 225) [69, 71, 72]

$3 -1602.47 0 23957.9 b71 (260, 225) [23, 70]

$3 -801.233 0 945.269 b72 (264, 186) [70]

$1 -9080.62 0 0 b73 (300, 258) [69, 74]

$1 -6276.33 0 0 b74 (314, 265) [68, 69, 73, 76, 117]

$1 -9080.62 0 0 b75 (347, 262) [76, 117]

$1 -8145.87 0 0 b76 (372, 273) [68, 74, 75, 77, 79, 81]

$1 -9481.29 0 0 c77 (381, 253) [76, 78]

$1 -5208.01 0 0 c78 (397, 247) [77, 79]

$3 -17360.1 29043.6 29043.6 c79 (424, 268) [76, 78, 80, 95, 96, 97, 98]

$1 -1602.47 0 0 c80 (428, 253) [67, 79]

$1 -7211.1 0 0 c81 (354, 303) [76, 82, 95]

$1 -2670.78 0 0 c82 (344, 323) [81, 83, 84]

$1 -1468.93 0 0 c83 (329, 331) [82, 84]

$1 -3204.93 0 0 c84 (330, 344) [82, 83, 85, 87, 88]

$1 -2804.32 0 0 c85 (320, 366) [84, 86]

$2 0 1.31034 1.31034 c86 (308, 394) [85]

$1 -6409.86 0 0 c87 (345, 347) [84, 88]

$2 0 23731.6 23731.6 c88 (370, 351) [84, 87, 89, 91]

$3 -21766.8 0 24523.4 c89 (388, 383) [88, 90]

$3 -1335.39 31028.5 31028.5 c90 (404, 370) [89, 91]

$1 -8680.03 0 0 c91 (411, 354) [88, 90, 92, 93, 99, 101]

$1 -1602.47 0 0 c92 (412, 339) [91, 93]

$1 -4006.16 0 0 c93 (428, 320) [91, 92, 94, 95, 99]

$1 -5608.63 0 0 c94 (413, 318) [93, 95]

$1 -5074.47 0 0 c95 (391, 308) [79, 81, 93, 94, 96]

$1 -2003.09 0 0 c96 (406, 290) [79, 95]

$1 -4540.32 0 0 c97 (437, 289) [79, 99]

$3 -5608.63 23898.2 27694.3 c98 (451, 297) [79, 99]

$3 -4940.94 19920.6 19920.6 c99 (465, 321) [91, 93, 97, 98, 100, 102, 103, 105]

$1 -2937.85 0 0 c100 (452, 356) [99, 101]

$1 -667.694 0 0 c101 (427, 360) [91, 100]

$3 -3071.39 25694.1 25694.1 c102 (496, 353) [99, 103, 104, 109]

$1 -5074.47 0 0 c103 (516, 323) [99, 102, 104]

$1 -4139.7 0 0 c104 (535, 321) [102, 103, 105, 106, 107]

$1 -5742.17 0 0 c105 (548, 310) [99, 104, 106]

$3 -6676.94 0 9760.98 c106 (575, 319) [104, 105]

$1 -267.078 0 0 c107 (539, 334) [104, 108]

$1 -1068.31 0 0 c108 (534, 349) [107, 109]

$1 -5208.01 0 0 c109 (532, 363) [102, 108, 110, 111]

$2 0 1.3802 1.3802 c110 (531, 376) [109]

$3 -9080.62 13095.9 13095.9 c111 (558, 376) [109]

$3 -801.233 33263.4 33263.4 a112 (118, 148) [16, 31]

$1 -1068.31 0 0 a113 (112, 213) [31, 114]

$1 -2937.85 0 0 a114 (130, 213) [26, 113]

$3 -24571.2 28575.4 28575.4 b115 (333, 234) [67]

$1 -2670.78 0 0 a116 (152, 38) [11]

$1 -4406.78 0 0 b117 (333, 265) [74, 75]

// 0 1 0.0999 4667.71 1

0 2 0.0424 7713.04 1

1 11 0.0616 8744.93 1

2 4 0.108 13197.6 1

2 11 0.16 4445.26 1

3 4 0.00798 20323.6 1

3 10 0.0688 12745.3 1

4 5 0.054 15822 1

4 7 0.0267 47831.1 1

4 10 0.0682 12308.4 1

5 6 0.0208 5557 1

6 11 0.034 6169.97 1

7 8 0.0305 2675.34 1

7 29 0.0504 41143.2 1

8 9 0.0322 5.97851 1

10 11 0.0196 9845.9 1

10 12 0.0731 7553.31 1

11 13 0.0707 7876.19 1

11 15 0.0834 8042.71 1

11 116 0.14 4445.27 1

12 14 0.2444 7713.04 1

13 14 0.195 8212.8 1

14 16 0.0437 28605.2 1

14 18 0.0394 7931.28 1

14 32 0.1244 17083.8 1

15 16 0.1801 13014.8 1

16 17 0.0505 18836.4 1

16 29 0.0388 30610.7 1

16 30 0.1563 19779 1

16 112 0.0301 40857.3 1

17 18 0.0493 10631.2 1

18 19 0.117 7659.43 1

18 33 0.247 16730.1 1

19 20 0.0849 9575.01 1

20 21 0.097 12394.5 1

21 22 0.159 14551.5 1

22 23 0.0492 44115.7 1

22 24 0.08 22098 1

22 31 0.1153 22740.2 1

23 69 0.4115 25782.4 1

23 71 0.196 23059.6 1

24 25 0.0382 23878.1 1

24 26 0.163 16486 1

25 29 0.086 39624.6 1

26 27 0.0855 8929.82 1

26 31 0.0755 10195.4 1

26 114 0.0741 7500.8 1

27 28 0.0943 6169.96 1

28 30 0.0331 9182.54 1

29 37 0.054 74960.6 1

30 31 0.0985 9508.43 1

31 112 0.203 12053.5 1

31 113 0.0612 5794.52 1

32 36 0.142 16156.5 1

33 35 0.0268 7143.34 1

33 36 0.0094 23221 1

33 42 0.1681 16156.6 1

34 35 0.0102 2904.69 1

34 36 0.0497 7606.19 1

36 37 0.0375 34464.8 1

36 38 0.106 17814.1 1

36 39 0.168 18968.3 1

37 64 0.0986 68411.3 1

38 39 0.0605 22582.1 1

39 40 0.0487 18968.3 1

39 41 0.183 13383.1 1

40 41 0.135 13761.7 1

41 48 0.1615 27818 1

42 43 0.2454 12481.3 1

43 44 0.0901 13105.8 1

44 45 0.1356 13197.6 1

44 48 0.186 8867.78 1

45 46 0.127 10856 1

45 47 0.189 6995.41 1

46 48 0.0625 9642.08 1

46 68 0.2778 12394.6 1

47 48 0.0505 6388.95 1

48 49 0.0752 12308.4 1

48 50 0.137 15173.5 1

48 53 0.145 18446.3 1

48 65 0.04595 33987.3 1

48 68 0.324 11399.3 1

49 56 0.134 8867.83 1

50 51 0.0588 6478.72 1

50 57 0.0719 5518.38 1

51 52 0.1635 2945.5 1

52 53 0.122 4476.38 1

53 54 0.0707 3920.73 1

53 55 0.00955 17938.8 1

53 58 0.2293 5480.02 1

54 55 0.0151 8992.36 1

54 58 0.2158 6300.45 1

55 56 0.0966 6755.63 1

55 57 0.0966 3975.81 1

55 58 0.12243 10557.3 1

58 59 0.145 9055.33 1

58 60 0.15 10780.5 1

58 62 0.0386 33818.2 1

59 60 0.0135 24535.5 1

59 61 0.0561 4700.39 1

60 61 0.0376 10780.5 1

60 63 0.0268 26884.4 1

61 65 0.218 8155.71 1

61 66 0.117 5714.24 1

62 63 0.02 36009.4 1

63 64 0.0302 61186.6 1

64 65 0.037 37576.5 1

64 67 0.016 86786.5 1

65 66 0.1015 11163.2 1

67 68 0.037 26697.6 1

67 80 0.0202 74960.7 1

67 115 0.00405 38611 1

68 69 0.127 17814.1 1

68 74 0.122 17083.9 1

68 76 0.101 38639.7 1

69 70 0.0355 34080.2 1

69 73 0.1323 17938.7 1

69 74 0.141 18705.5 1

70 71 0.18 36036.2 1

70 72 0.0454 1240.23 1

73 74 0.0406 11886.5 1

74 76 0.1999 13571 1

74 117 0.0481 19101 1

75 76 0.148 16613.7 1

75 117 0.0544 13955 1

76 77 0.0124 21060.5 1

76 79 0.033176 26492.3 1

76 81 0.0853 32912.1 1

77 78 0.0244 7193.34 1

78 79 0.0704 10483.9 1

79 80 0.037 72391.2 1

79 95 0.182 15822 1

79 96 0.0934 17445.2 1

79 97 0.108 18968.2 1

79 98 0.206 24898.7 1

81 82 0.03665 20914.1 1

81 95 0.053 12656.6 1

82 83 0.132 8155.72 1

82 84 0.148 11163.2 1

83 84 0.0641 8929.84 1

84 85 0.123 4635.26 1

84 87 0.102 11085.6 1

84 88 0.173 12924.3 1

85 86 0.2074 1.41869 1

87 88 0.0712 15810.3 1

88 89 0.06515 23529.8 1

88 91 0.038274 20283.2 1

89 90 0.0836 21506 1

90 91 0.1272 21208 1

91 92 0.0848 11559.4 1

91 93 0.158 11085.6 1

91 99 0.295 6524.07 1

91 101 0.0559 6755.63 1

92 93 0.0732 10705.6 1

93 94 0.0434 19779 1

93 95 0.0869 19917.5 1

93 99 0.058 27262.1 1

94 95 0.0547 16613.7 1

95 96 0.0885 14450.3 1

97 99 0.179 18575.4 1

98 99 0.0813 27645.2 1

99 100 0.1262 8806.17 1

99 102 0.0525 24880.2 1

99 103 0.204 10195.4 1

99 105 0.229 10780.5 1

100 101 0.112 6388.96 1

102 103 0.1584 8684.14 1

102 104 0.1625 10266.8 1

102 109 0.1813 15386.6 1

103 104 0.0378 9777.46 1

104 105 0.0547 5794.52 1

104 106 0.183 5875.93 1

104 107 0.0703 8386.48 1

105 106 0.183 5075.25 1

107 108 0.0288 7931.28 1

108 109 0.0762 6344.55 1

109 110 0.0755 1.48968 1

109 111 0.064 13105.8 1

113 114 0.0104 4833.38 1

BIBLIOGRAPHY

[1] K.B. Athreya, P.E. Ney, *Branching Processes*, Dover NY 2004 (reprint of Springer-verlag Berlin 1972).

[2] N. Becker, Estimation for Discrete Time Branching Processes with Application to Epidemics, *Biometrics*, Vol 33, No 3, pp.512-522, 1977.

[3] V.M. Bier, E.R. Gratz, N.J. Haphuriwat, W. Magua, K.R. Wierzbicki, Methodology for Identifying Near-Optimal Interdiction Strategies for a Power Transmission System, *Workshop on Safeguarding National Infrastructures*, Glasgow, UK, 2005.

[4] B.A. Carreras, V.E. Lynch, I. Dobson, D.E. Newman, Critical points and transitions in an electric power transmission model for cascading failure blackouts, *Chaos*, vol. 12, no. 4, December 2002, pp. 985-994.

[5] B.A. Carreras, V.E. Lynch, I. Dobson, D.E. Newman, Dynamical and probabilistic approaches to the study of blackout vulnerability of the power transmission grid, *37th Hawaii International Conference on System Sciences*, Hawaii, 2004.

[6] B.A. Carreras, V.E. Lynch, I. Dobson, D.E. Newman, Complex dynamics of blackouts in power transmission systems, *Chaos*, vol. 14, no. 3, September 2004, pp. 643-652.

[7] B.A. Carreras, D.E. Newman, I. Dobson, A.B. Poole, Evidence for self organized criticality in a time series of electric power system blackouts, *IEEE Transactions on Circuits and Systems I*, vol. 51, no. 9, September 2004, pp. 1733-1740.

[8] Q. Chen, J.D. McCalley, A cluster distribution as a model for estimating high-order event probabilities in power systems, *Eighth International Conference on Probability Methods Applied to Power Systems*, Ames Iowa, September 2004.

[9] J. Chen, J.S. Thorp, I. Dobson, Cascading dynamics and mitigation assessment in power system disturbances via a hidden failure model, *International Journal of Electrical Power and Energy Systems*, Vol 27, No 4, 2005, pp. 318-326.

[10] P.C. Consul, *Generalized Poisson Distributions: Properties and Application*, Marcel Dekker, NY, 1989.

[11] J.-P. Dion, N. Keiding, Statistical inference in branching processes, in *Branching Processes*, editors A. Joffe, P. Ney, Marcel Dekker, New York 1978, pp. 105-140.

[12] J.P. Dion, N.M. Yanev, Statistical inference for branching processes with an increasing random number of ancestors, *Journal of Statistical Planning and Inference*, vol 39, 1994, pp. 329-352.

[13] I. Dobson, B.A. Carreras, D.E. Newman, Probabilistic load-dependent cascading failure with limited component interactions, *IEEE International Symposium on Circuits and Systems*, Vancouver Canada, May 2004.

[14] I. Dobson, B.A. Carreras, V.E. Lynch, B. Nkei, D.E. Newman, Estimating failure propagation in models of cascading blackouts, *Eighth International Conference on Probability Methods Applied to Power Systems*, Ames Iowa, September 2004 and *Probability in the Engineering and Informational Sciences*, vol. 19, no. 4, October 2005, pp 475-488.

[15] I. Dobson, B.A. Carreras, D.E. Newman, A branching process approximation to cascading load-dependent system failure. *37th Hawaii International Conference on System Sciences*, Hawaii, January 2004.

[16] I. Dobson, B.A. Carreras, D.E. Newman, Branching process models for the exponentially increasing portions of cascading failure blackouts, *38th Hawaii International Conference on System Sciences*, January 2005, Hawaii.

[17] I. Dobson, K.R. Wierzbicki, B.A. Carreras, V.E. Lynch, D.E. Newman, An estimator of propagation of cascading failure, *39th Hawaii International Conference on System Sciences*, January 2006, Kauai, Hawaii.

[18] I. Dobson, B.A. Carreras, D.E. Newman, A loading-dependent model of probabilistic cascading failure, *Probability in the Engineering and Informational Sciences*, vol. 19, no. 1, January 2005.

[19] Electricity Consumers Resource Council, *The Economic Impacts of the August 2003 Blackout*, February 2004.

[20] M.J. Feigenbaum, Quantitative universality for a class of nonlinear transformations, *Journal of Statistical Physics*, Vol 19, No 1, 1978, pp. 25-52.

[21] M.J. Feigenbaum, Universal metric properties of nonlinear transformations, *Journal of Statistical Physics*, Vol 21, No 6, 1979, pp. 669-706.

[22] W. Feller, *An introduction to probability and its applications*, Volume 1, third edition, John Wiley, NY, 1968.

[23] P. Grassberger, Temporal scaling at feigenbaum points and non-extensive thermodynamics, *Archiv e-print*, cond-mat:0508110, 2005.

[24] P. Guttorp, *Statistical inference for branching processes*, Wiley, NY, 1991

[25] R.C. Hardiman, M.T. Kumbale, Y.V. Makarov, An advanced tool for analyzing multiple cascading failures, *Eighth International Conference on Probability Methods Applied to Power Systems*, Ames Iowa, September 2004.

[26] T.E. Harris, *Theory of branching processes*, Dover NY 1989.

[27] B. Hu, J. Rudnick, Exact solutions to the feigenbaum renormalization-group equations for intermittency, *Physical Review Letters*, Vol 48, No 24, 1982, pp.1645-1648.

[28] P.J.M. Kallenburg, *Branching processes with continuous state space*, Mathematical Centre Tracts 117, ISBN 90 6196 188 2, Amsterdam 1979

[29] D.S. Kirschen, D. Jawayeera, D.P. Nedic, R.N. Allan, A probabilistic indicator of system stress, *IEEE Transactions on Power Systems*, vol. 19, no. 3, 2004, pp. 1650-1657.

[30] D.P. Nedic, I. Dobson, D.S. Kirschen, B.A. Carreras, V.E. Lynch, Criticality in a cascading failure blackout model, *Fifteenth Power Systems Computation Conference*, Liege Belgium, August 2005, and to appear in International Journal for Electric Energy and Power Systems.

[31] R. Otter, The Multiplicative Process, *The Annals of Mathematical Statistics*, Vol 20, No 2, June 1949, pp. 206-224.

[32] S.M. Rinaldi, J.P. Peerenboom, T.K. Kelly, Identifying, understanding, and analyzing critical infrastructure interdependencies, *IEEE Control Systems Magazine*, December 2001, pp. 11-25.

[33] A. Robledo, Criticality in non-linear one-dimensional maps: RG universal map and non-extensive entropy, *Arxiv e-print*, cond-mat:0202095, 2003.

[34] S. Roy, C. Asavathirathan, B.C. Lesieutre, G.C. Verghese, Network models: gorwth, dynamics, and failure, *34th Hawaii International Conference on System Sciences*, 2001.

[35] A. Saichev, A. Helmstetter, D. Sornette, Power Law Distributions of Offspring and Generation Numbers in Branching Process Models of Earthquake Triggering, *Archiv e-print*, cond-mat:0305007, 2006.

[36] E. Seneta, D. Vere-Jones, On the asymptotic behaviour of subcritical branching processes with continuous state space, *Zeitschrift fur Wahrscheinlichkeitstheorie und verwandte Gebiete*, vol. 10, pp. 212-225, 1968.

[37] J.C. Sprott, *Chaos and Time Series Analysis*, Oxford University Press, 2003.

[38] H.M. Srivastava, H.L. Manocha, *A Treatise on Generating Functions*, Ellis Horwood, Chichester, UK 1984

[39] U.S.-Canada Power System Outage Task Force, *Final Report on the August 14th blackout in the United States and Canada*. United States Department of Energy and National Resources Canada, April 2004.

[40] R. Tonelli, Convergence to the critical attractor at infinite and tangent bifurcation points, *Archiv e-print*, nlin.CD:0509030, 2005.

[41] C. Tsallis, F.Baldovin, R. Cerbino, P. Pierobon, Introduction to nonextensive statistical mechanics and thermodynamics, *Archiv e-print* cond-mat:0309093, 2005.

[42] V.K. Tuan, D.T. Duc, Convergence rate of Post-Widder approximate inversion of the Laplace transform, *Vietnam Journal of Mathematics*, Vol 28, No 1, 2000, pp. 93-96.

[43] V. Venkatasubramanian, J. Quintero, *Detection, Prevention, and Mitigation of Cascading Events: Part II of the Final Project Report*, Power Systems Engineering Research Center, November 2005.

[44] V. Vittal, X. Wang, *Detection, Prevention, and Mitigation of Cascading Events: Part III of the Final Project Report*, Power Systems Engineering Research Center, October 2005.

[45] E.T. Whittaker, G.N. Watson, *A Course of Modern Analysis*, Cambridge University Press, Cambridge, UK, 1948.

[46] D.V. Widder, *The Laplace Transform*, Princeton University Press, Princeton, NJ, 1946.

[47] K.R. Wierzbicki, I. Dobson, An approach to statistical estimation of cascading failure propagation in blackouts, preprint to appear at *CRIS, Third International Conference on Critical Infrastructures*, Alexandria, VA, September 2006.

[48] N.M. Yanev, On the Statistics of Branching Processes, *Theory of Probability and its Applications*, Vol 20, 1975, pp. 612-622.

[49] R. Zimmerman, C.E. Restrepo, The next step: quantifying infrastructure interdependencies to improve security, *International Journal of Critical Infrastructures*, vol. 2, nos. 2/3, 2006